A Novel Approach to Breast Tumor Classification

By

Mehwish Ikram Mughal

(Registration No: 00000362273)

Department of Computing

School of Electrical Engineering and Computer Science

National University of Sciences & Technology (NUST)

Islamabad, Pakistan

(2023)

A Novel Approach to Breast Tumor Classification

By

Mehwish Ikram Mughal

(Registration No: 00000362273)

A thesis submitted to the National University of Sciences and Technology, Islamabad,

in partial fulfillment of the requirements for the degree of

Master of Science in

Computer Science

Supervisor: Dr. Arbab Latif

Co Supervisor: Dr. Shahzad Younas,

Dr. Muhammad Imran

School of Electrical Engineering and Computer Science

National University of Sciences & Technology (NUST)

Islamabad, Pakistan

(2023)

THESIS ACCEPTANCE CERTIFICATE

Certified that final copy of MS/MPhil thesis entitled "A Novel Approach to Breast Tumor Classification" written by Mehwish Ikram Mughal, (Registration No 00000362273), of SEECS has been vetted by the undersigned, found complete in all respects as per NUST Statutes/Regulations, is free of plagiarism, errors and mistakes and is accepted as partial fulfillment for award of MS/M Phil degree. It is further certified that necessary amendments as pointed out by GEC members of the scholar have also been incorporated in the said thesis.

Signature: _____

Name of Advisor: Dr. Arbab Latif

Date: 15-Feb-2024

HoD/Associate Dean: _____

Date: 18 Mar 2024

Signature (Dean/Principal): _____

Date: 18 Mar 2024

Dr. Muhammad Ajmal
Principal
NUST School of Electrical Engineering & Computer Science
Sector H-12, Islamabad

Publish Date & Time: Thursday, 15 February 2024 , 15:48:35

FORM TH-4

National University of Sciences & Technology

MASTER THESIS WORK

We hereby recommend that the dissertation prepared under our supervision by: (Student Name & Reg. #) Mehwish Ikram Mughal [00000362273]

Titled: A Novel Approach to Breast Tumor Classification

be accepted in partial fulfillment of the requirements for the award of Master of Science (Computer Science) degree.

Examination Committee Members

1. Name: Muhammad Imran Signature: 12-Mar-2024 1:31 PM

2. Name: Muhammad Shahzad Younis Signature: 12-Mar-2024 1:31 PM

Supervisor's name: Arbab Latif Signature: 13-Mar-2024 9:58 AM

HoD/Associate Dean — Date: 18 Mar 2024

COUNTERSINGED

Date: 18 Mar 2024 — Dean/Principal

Online Printing Date & Time: Friday, 16 February 2024 01:34:53

Approval

It is certified that the contents and form of the thesis entitled "A Novel Approach to Breast Tumor Classification" submitted by Mehwish Ikram Mughal have been found satisfactory for the requirement of the degree

Advisor : Dr. Arbab Latif

Signature: _____

Date: 15-Feb-2024

Committee Member 1:Dr Muhammad Imran

Signature: _____

14-Feb-2024

Committee Member 2:Dr. Muhammad Shahzad Younis

Signature: _____

Date: 14-Feb-2024

Thesis Printing Date & Time: Friday, 16 February 2024 01:55:31

Certificate of Originality

I hereby declare that this submission titled "A Novel Approach to Breast Tumor Classification" is my own work. To the best of my knowledge it contains no materials previously published or written by another person, nor material which to a substantial extent has been accepted for the award of any degree or diploma at NUST SEECS or at any other educational institute, except where due acknowledgement has been made in the thesis. Any contribution made to the research by others, with whom I have worked at NUST SEECS or elsewhere, is explicitly acknowledged in the thesis. I also declare that the intellectual content of this thesis is the product of my own work, except for the assistance from others in the project's design and conception or in style, presentation and linguistics, which has been acknowledged. I also verified the originality of contents through plagiarism software.

Student Name:Mehwish Ikram Mughal

Student Signature: _____

Publish Date & Time: Thursday, 15 February 2024 , 15:4

Certificate for Plagiarism

It is certified that PhD/M.Phil/MS Thesis Titled "A Novel Approach to Breast Tumor Classification" by Mehwish Ikram Mughal has been examined by us. We undertake the follows:

a. Thesis has significant new work/knowledge as compared already published or are under consideration to be published elsewhere. No sentence, equation, diagram, table, paragraph or section has been copied verbatim from previous work unless it is placed under quotation marks and duly referenced.
b. The work presented is original and own work of the author (i.e. there is no plagiarism). No ideas, processes, results or words of others have been presented as Author own work.
c. There is no fabrication of data or results which have been compiled/analyzed.
d. There is no falsification by manipulating research materials, equipment or processes, or changing or omitting data or results such that the research is not accurately represented in the research record.
e. The thesis has been checked using TURNITIN (copy of originality report attached) and found within limits as per HEC plagiarism Policy and instructions issued from time to time.

Name & Signature of Supervisor

Dr. Arbab Latif

Signature : Latif

Publish Date & Time: Thursday, 15 February 2024 , 15:4

DEDICATION

Dedicated

To

My beloved Father

Muhammad Ikram Mughal

Who believed in me when things look bleak and who is the reason

behind my all struggles.

My Marvelous Mother

Shaheen Akhtar

Whose kind prayers and support with guidance throughout my

career never let me stray away.

My Best Friend

& Myself

Acknowledgements

Glory be to Allah (S.W.A), the Creator, the Sustainer of the Universe. Who only has the power to honor whom He please, and to abase whom He please. Verily no one can do anything without His will. From the day, I came to NUST till the day of my departure, He was the only one Who blessed me and opened ways for me, and showed me the path of success. Their is nothing which can payback for His bounties throughout my research period to complete it successfully.

Mehwish Ikram Mughal

TABLE OF CONTENTS

ACKNOWLEDGEMENTS **VII**

TABLE OF CONTENTS **VIII**

LIST OF TABLES **XI**

LIST OF FIGURES **XII**

LIST OF ABBREVIATIONS **XIV**

ABSTRACT **XV**

CHAPTER 1: INTRODUCTION **1**

1.1 Overview 1

1.2 Cancer 2

1.3 Breast Cancer 2

1.4 Purpose of Study 7

1.5 Proposed Work 8

1.6 Summary 8

CHAPTER 2: BACKGROUND 9

2.1 Overview 9

2.2 Breast Cancer 10

2.3 Evolution of BC from Ancient Beliefs to Modern Breakthroughs 11

2.4 Diagnostic Techniques 14

2.4.1 Mammography 14

2.4.1.1 Mammography Procedure 15

2.4.1.2 Mammography Pros 15

2.4.1.3 Mammography Cons 15

2.4.2 Breast Ultrasound 15

2.4.2.1 Breast Ultrasound Procedure 16

2.4.2.2 Breast Ultrasound Pros 16

2.4.2.3 Breast Ultrasound Cons 16

2.4.3 Breast MRI 16
2.4.3.1 Breast MRI Procedure 16
2.4.3.2 Breast MRI Pros 17
2.4.3.3 Breast MRI Cons 17
2.4.4 Biopsy 17
2.4.4.1 Biopsy Procedure 18
2.4.4.2 Types of Biopsy Procedure 18
2.5 Challenges and Limitations in terms of efficiency and accuracy 18
2.6 Computer Aided Diagnosis 19
2.7 CAD using histopathological images BC diagnosis 20
2.7.1 Step 1 Preprocessing 20
2.7.2 Step 2 Segmentation 21
2.7.3 Step 3 Feature Extraction 21
2.7.4 Step 4 Classification 22
2.8 Summary 23

CHAPTER 3: LITERATURE REVIEW 24

3.1 Overview 24
3.2 Comparison of conventional Computer Vision and Deep Learning 25
3.3 Exploring conventional technique for Breast Cancer classification 26
3.4 Exploring Deep Learning techniques for BC classification 29
3.5 Summary 44

CHAPTER 4: METHODOLOGY 45

4.1 Overview 45
4.2 Data Collection 45
4.2.1 Dataset 46
4.2.2 Dataset Limitation 50
4.2.3 Dataset Advantage 50
4.3 Preprocessing 51

4.3.1 Down Sampling 51
4.3.2 Splitting 52
4.3.3 Resizing 53
4.3.4 Augmentation 53
4.3.5 Balancing 54
4.4 Proposed Model 54
4.4.1 YOLO 55
4.4.2 Modified Yolo Architecture 57
4.5 Training Process 58
4.6 Summary 60

CHAPTER 5: RESULTS AND DISCUSSION 61

5.1 Experimental Setup 61
5.2 Evaluation Metrics 62
5.3 Experimental Results 62
5.4 Discussion 66

CHAPTER 6: CONCLUSION 68

REFERENCES 70

LIST OF TABLES

Page No.

Table 3.1: Comparison of ML methods design for BC diagnosis 38

Table 3.2: Comparison of DL methods design for BC diagnosis 39

Table 3.3: ML and DL hybrid models comparison for BC diagnosis 42

Table 4.1: Distribution of BreaKHis dataset 48

Table 5.1: Experimental setup 61

Table 5.2: Breast cancer classification results comparison 67

LIST OF FIGURES

Page No.

Fig 1.1: Breast cancer rate in Pakistan 4

Fig 1.2: Breast cancer in females 5

Fig 2.1: Evolution of Breast cancer 14

Fig 2.2: CAD system components 22

Fig 3.1: Deep Learning and Computer Vision workflow 26

Fig 4.1: Sample from BreaKHis Dataset 46

Fig 4.2: Examples of images with labels from the BreaKHis with several magnification levels 47

Fig 4.3: Ductal carcinoma from same slide 14-2523 at four different magnifications 47

Fig 4.4: Folder structure of Dataset 49

Fig 4.5: Dataset Classes 51

Fig 4.6: Preprocessing steps workflow 52

Fig 4.7: Dataset splitting 52

Fig 4.8: Splitting according to Zoom size 53

Fig 4.9: Augmentation techniques 54

Fig 4.10: Workflow of proposed methodology 54

Fig 4.11: Modified architecture of YOLOv5 57

Fig 4.12: Result image with class probabilities 59

Fig 5.1: Confusion Matrix 62

Fig 5.2: Binary class Accuracy 63

Fig 5.3: Binary class Confusion matrix 63

Fig 5.4: Malignant class accuracy graph 64

Fig 5.5: Malignant class Confusion matrix 64

Fig 5.6: Benign class Accuracy Graph 65

Fig 5.7: Benign class Confusion matrix 65

LIST OF ABBREVIATIONS

BC	Breast Cancer
HI	Histopathological imaging
AI	Artificial Intelligence
WCRF	World Cancer Research Fund
WHO	World Health Organization
IARC	International Cancer Research Center
MRI	Magnetic resonance imaging
CAD	Computer-Aided Diagnosis
AI	Artificial intelligence
ML	Machine Learning
DL	Deep Learning
CV	Computer Vision
YOLO	You Only Look Once
CNN	Convolutional Neural Network
BN	Batch Normalization
1D	One Dimensional

ABSTRACT

Microscopic examination is essential for Breast cancer which is the most common cancer among women worldwide. Finding clinical assessment hints to make accurate diagnoses during a pathology examination involves laboriously going through tissue photos at various magnification levels. Experts may also disagree as a result of personally examining breast cancer cases. Technological developments in digital imaging allow for the evaluation of pathology pictures through the use of computer vision and deep learning techniques, potentially automating a number of jobs within the diagnostic pathology process. Reducing observer variability, increasing objectivity, and obtaining quick and accurate quantification might all be facilitated by such automation. While deep learning techniques provide remarkable results in classification tasks involving histopathology pictures of breast cancer, current state-of-the-art algorithms are either computationally costly or only distinguish between binary or multi classes. Models that combine both binary and multiclass classification do not outperform ours model for multiclass in terms of performance accuracy. Furthermore, a small number of current models that achieve high performance accuracy are dependent on different magnification factors, rendering the model dependent.

Our primary contribution to this work is the implementation of the YOLOv5 (You Only Look Once) model with ResNet feature extractor, which is built on the CSP-Darknet53 backbone with the ResNet block incorporated after its backbone in order to extract complex hierarchical features from histopathological images for Breast Cancer classification. Additionally, we trained the model using images from all magnification factors, which makes it independent from magnification and increases its generalizability. It can detect BC from images acquired at various magnifications (10X, 200X, 400X, and 100X). Experiments indicate that an 80% and 20% ratio of training testing yields the optimum accuracy performance. The suggested model has a 99% binary class accuracy, a 98% malignant class accuracy, and a 97% benign class accuracy.

Keywords: Breast Cancer, Classification, Histopathological images, Resnet, YOLO.

CHAPTER 1

Introduction

1.1 Overview:

Breast cancer (BC) is caused by aberrant growth of cells that results in benign or malignant tumors in the breast. Effective therapy depends on early discovery achieved by self-examination and medical exams. BC is still a major issue in the world today, despite progress, and Pakistan is particularly challenged because of cultural differences. For patients with BC, an early and accurate diagnosis is critical to improving their prognosis and increasing their survival rate by 30% to 50%. When compared to other imaging modalities, histopathological imaging (HI) is more often utilized for the identification of BC. Nevertheless, there are three main drawbacks to manual histopathology image analysis. Firstly, in many underdeveloped nations, there is a dearth of experienced pathologists in healthcare institutions. Second, pathologists find the process laborious and time-consuming. As a result, pathologists working on picture analysis may become tired and pay less attention. Ultimately, artificial intelligence-driven automated solutions are becoming essential for precise and timely BC diagnosis. Therefore, computer-aided diagnostic methods might be utilized as a second opinion to examine the histopathological pictures for BC in order to solve the aforementioned constraints.

1.2 Cancer:

Despite remarkable current advances in diagnosis and treatment, cancer continues constituting a massive public health problem around the world. Hippocrates who is known as “Father of Medicine” [1] was the first who used the term "cancer" about 400 BCE, and according to his explanation it was caused by an imbalance of the body's humors, which include black bile, blood, yellow bile, and phlegm [2]. This was a pioneering effort to comprehend the illness.

Cancer is defined as group of disorders characterized by excessive cell multiplication and its dissemination throughout the body. The human body's regular cells divide to produce new cells when the body needs them for maintenance or replacement. Normal cells eventually die, while malignant cells behave improperly because of cell mutations that push out normal cells [1]. These cells have the ability to infiltrate and kill healthy tissues and organs, leading to life-threatening illnesses or even death if treatment is not provided. It emerges when genetic anomalies occur in healthy cells, leading to malfunctions in the mechanisms governing cell division and proliferation.

These mutations can be hereditary or picked up over the course of a person's lifetime due to a number of different conditions, including exposure to carcinogens (such as tobacco smoke, certain chemicals, exposure to radiation), persistent inflammation, or specific infections. Cancer remains a major global public health concern despite amazing recent advancements in detection and treatment. As reported by the World Cancer Research Fund (WCRF), there has been a 20% increase in the past ten years, and until 2030, 27 million more instances of this illness are expected to occur [3]. There are several more types of cancer, including lung, colorectal, prostate, and breast cancer. Different medicines are required for each form of cancer due to their distinct behaviors.

1.3 Breast Cancer:

One of the deadliest kinds of cancer and one of the most prevalent is BC. Both males and females can be diagnosed with this disease, but most commonly females are diagnosed with this type of cancer. In United States, BC is the second most common leading cancer in women. Approximately 1 in 8 women and 1 in 833 men in the U.S may get invasive BC at some point in their lives [4].

BC arises from the uncontrolled growth and reproduction of abnormal cells in the breast, which lead to the formation of a tumor that can infiltrate surrounding tissues and spread to other parts of the body. The breast is composed of three main components: lobules, ducts, and connective tissue. The lobules act as the milk-producing glands, the ducts are the tubes that carry milk to the nipple, and the connective tissue holds everything together and forms the actual breast. Usually, in BC cancerous cells begin to grow in the lobules and ducts. Most often, BC grows to other areas of an impacted breast, then to the lymph nodes nearby. If cancerous cells manage to enter the lymphatic system, they may extend to other body parts.

BC is highly deadly and prevalent. Breast lumps and changes in breast size and form are among the symptoms of BC. Irregular growth of cells in the breast forms a mass or lump which is basically called tumor. It usually develops when cells do either proliferate beyond the natural limits or they fail to die when they should ought to. This tumor can be categorized in two types. Depending on important factors likewise size, perimeter, density, gradient, and texture, a tumor may be malignant (cancerous) or benign (non-cancerous) [5].

A non-cancerous cell growth in the breast is called a benign breast tumor. They are often "innocent," slow-growing, confined, and do not infiltrate adjacent tissues or spread to other regions of the body, they are frequently assumed to be innocuous when found in breast tissue. Even while it could get bigger, it usually doesn't endanger life. Benign tumors don't spread malignancy. They are incapable of invading neighboring tissues or spreading to other organs [6].

They are frequently find enclosed, that is, inside a clearly defined limit or capsule. They are non-invasive because of this confinement. These cells act similarly to normal cells. Compared to malignant cells, they usually show less change in size and form. While some can only be found through imaging testing, others may feel like a lump in the breast. Under a microscope, they may have a more consistent and uniform look and develop more slowly. The course of treatment differs and may include surgical excision of big or symptomatic tumors, aspiration of cysts, or observation.

A malignant breast tumor poses a greater risk to one's health since it is cancerous, which means it can spread to other regions of the body and invade surrounding tissues. It calls for immediate and thorough medical attention. It is more dangerous because it can migrate to other regions of the body, develops more quickly, and invades nearby tissues. Because they are invasive,

malignant tumors have the ability to invade nearby tissues [6], including lymph nodes and has the capacity to travel via the lymphatic or circulatory systems to other organs.

Malignant tumor cells frequently have aberrant characteristics, such as atypical sizes and shapes. They could also divide at a faster pace. Angiogenesis, the process of creating new blood vessels to feed nutrients and promote the fast development of cancer cells, is stimulated by cancer cells. They might show up as skin changes, nipple discharge, breast alterations, or lumps or thickenings in the breast. Usually, a mix of surgery, chemotherapy, radiation treatment, hormone therapy, or immunotherapy is used to treat malignant breast tumors. Tumor size, stage, and molecular features are among the variables that determine the particular therapy strategy.

The pink ribbon has evolved into the global representation of BC. From age of forty, every woman should get a medical examination and mammography every two years. A key factor in the early diagnosis of the illness is self-examination for breast abnormalities or lumps. An estimated 2,800 men and 297,790 women will receive an invasive BC diagnosis in 2023 [4]. The World Health Organization (WHO) projected that 19.3 million new cases of BC will be detected globally in 2025. Research indicates that 1 in 9 women will likely get BC at some time in their lives, and that 77% of invasive BC cases affect women over the age of 50. However, if the disease is detected early, survival rates are close to 90%.

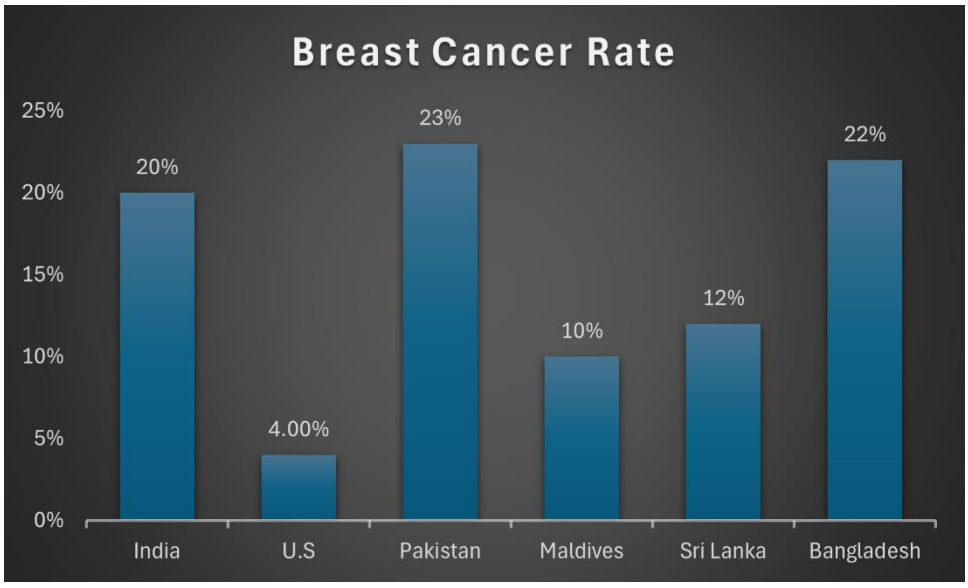

Fig: 1.1: Breast cancer rate in Pakistan

Cancer is a very concerning health issue in Pakistan as well. As seen in fig: 1.1, Pakistan had greater diagnosis rates for BC in 2020 when compared to other nations. Unfortunately, because of the shame associated with it, BC is not a significant topic of conversation in Pakistan. Over 83,000 instances of BC are thought to be recorded annually. Approximately 40,000 women in Pakistan lose their lives to this terrible illness each year [7]. Compared to the other cancer kinds in Pakistan illustrated in fig: 1.2, BC is the most common cancer in women in 2020.

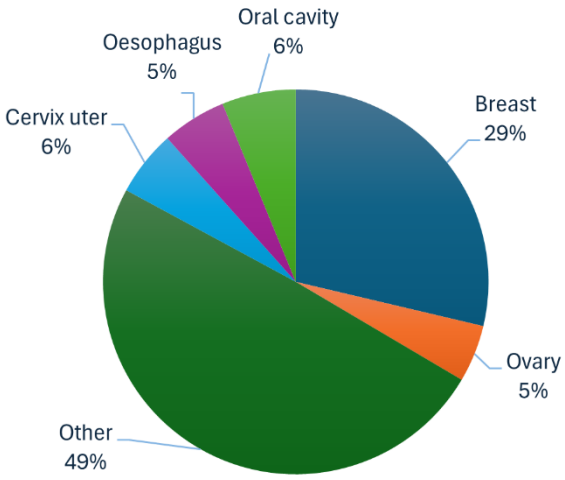

Fig 1.2: Breast cancer in females

Despite the fact that cancer is more common in industrialized nations, the death rate from the disease is comparatively greater in developing nations because of barriers to early detection and other limitations that impoverished women confront while trying to utilize advancements in medical technology. "Developing effective and affordable approaches to the early detection, diagnosis, and treatment of BC among women living in less developed countries is an urgent need in cancer control today," according to Dr. Christopher Wild, director of the International Cancer Research Center (IARC) [8].

Since at least 3,000 to 2,500 BCE, people have been aware of BC and have attempted to treat it. BC was usually identified back then by post-mortem autopsy or surgery. The development of more advanced techniques for detecting BC did not begin until the middle of the 1800s. Through the use of microscopy, various tumor kinds' cells may be examined in more depth, leading to more precise tumor diagnoses. Eventually, the first X-ray was taken in 1895, which paved the way for

the adoption of mammograms as a non-invasive way to image cancer [9]. It is now far easier to identify cancer early on and research its progression because to these technological advancements.

Due to its aggressiveness and high death rate BC is most prevalent type of cancer. It is impossible to exaggerate how crucial early and accurate diagnosis is to bettering patient outcomes and increasing survival rates. Early diagnosis can help medical professionals create customized treatment plans for patients based on the distinctive characteristics of the cancer. This might entail determining the best course of action, modifying dose, and employing targeted therapies based on the molecular profile of the malignancy. Also reducing the death rate requires early detection.

Current medical procedures include the use of effective screening and diagnosis methods including mammography, magnetic resonance imaging (MRI), CT scanning, and fine needle aspiration cytology (FNAC) to achieve early detection of BC. A lack of sensitivity for an in-depth assessment of cancerous areas and the identification of benign, malignant cancer subtypes is a drawback of current screening techniques. A biopsy is the only procedure that can accurately identify BC. During this invasive procedure, a small breast tissue sample is extracted to be examined under a microscope to determine if a suspicious area in the breast is benign or malignant (cancerous). This examination of the tissue's diseased area under a microscope for carcinogenic regions detection is referred as Histopathology.

The development of the microscope facilitated advancements in the study of histopathology. It is recognized as the gold standard in the diagnosis of tumors. Images from histopathology may be more sensitive to the differences between malignant and benign cancer subtypes. However, because histological images contain complex visual patterns, they are challenging for a pathologist to examine. Many patients are recommended for cancer biopsies at major hospitals, which generates vast amounts of complex data that are challenging for a human specialist to manage manually. Thus, automated techniques for BC subtype categorization are necessary.

Computer-Aided Diagnosis (CAD) systems have become common place in pathology laboratories' everyday operations due to factors including significant advancements in image processing algorithms, reduced storage costs, and significant increases in available computer power. As noted by Zewdie et al. [10], CAD technologies are desperately needed to reduce

pathologists' burden. Tumor pictures are quickly analyzed by CAD systems, which then divide them into groups that are malignant, benign and subgroups. Thus, these technologies offer a prompt and accurate diagnostic opinion, assisting the pathologist in making the ultimate decision.

Artificial intelligence (AI) is going to be extremely important in the diagnosis of cancer because it can analyze large amounts of data and spot trends that may be hard for human professionals to see. Digital tissue histopathology has recently become viable with the use of digital image analysis AI, and machine learning (ML) approaches. While digital microscopy has advanced, ML models have gained popularity for the detection of cancer. Using ML CAD model was created in 1993 by Street et al. [11]. In recent years, there has been a growing use of computer vision (CV) and deep learning (DL) techniques to medical image analysis, providing a powerful tool for BC detection and classification.

Survival rate can be increased by early detection and this will reduces the death rate which is crucial, but if detected early enough, 95% of instances of breast cancer are curable [12]. Given the evidence that a timely diagnosis may significantly lower the risk of dying from breast cancer, it is critical that diagnosis algorithms, like image classifiers, maintain becoming more accurate in order to prevent further declines in the number of deaths from BC. BC deaths may eventually come to an end if advances in early detection and diagnosis technology are maintained. In order to increase the number of lives saved from BC, this study explores the creation of an image classifier/CAD with the goal of increasing the accuracy diagnosis.

1.4 Purpose of Study:

The goal of this study is to create an automatic image classifier/CAD that can classify breast tumor is benign or malignant and can further divide the tumors into eight groups: four of which are benign and the other four of which are malignant, to support pathologists for BC classification job, reducing inter and intra expert variability and leading to a quicker, more objective, and consistent diagnosis. Image classification is assigning a whole image to one of a number of predetermined classes. Most of research conducted focuses either on binary classification but that’s not enough to get better insights or magnification dependent multiclass classification. By binary classification the identification and treatment of some aggressive subtypes of BC maybe delayed. Certain subtypes which exhibit fast advancement towards certain treatments, can require precise and quick

treatment. Subclassification is necessary in order to identify these aggressive subtypes quickly. Multiclassification aids in improved treatment planning and assessment of risk for pathologists and oncologists but magnification dependent models cannot perform in generic case. Many attempts have done for developing a more consistent and robust system for BC diagnosis. With this aim, the classifier in this study employs annotated histopathological pictures acquired from excisional biopsies since they are the most useful image type for categorizing tissues from publicly available Histopathological Image Classification (BreaKHis) dataset [6], which was created specifically with this goal in mind.

1.5 Proposed work:

We have developed an integrated magnification independent DL model, using proposed model You Only Look Once 5th variation (YOLOv5) with an additional ResNet block for learning for complex representations, for the classification of BC into benign, malignant classes and further sub type classification from Histopathological images. Using a publicly available dataset of BC cases, the efficiency of the proposed system is evaluated. We have also trained, evaluated and compared other models like ResNet50, InceptionV3, and InceptionResNetV2 performance with our proposed model. And found our model is outperforming these models.

Our main Contribution:

I. A modified YOLO model is proposed for magnification independent classification of Breast cancer and the findings demonstrate that our recommended method outperforms existing state-of-the-art procedures and achieves high accuracy.
II. As far as we are aware, no research has been done on the automated categorization of BC subclasses using the YOLOv5 model from histopathological photos.

1.6 Summary:

Section 1.2 highlights the disease of cancer and how deadly this disease is. Section 1.3 highlights about BC, how its affecting world widely. What advancements are being used for diagnosis of BC and the role of AI in cancer diagnosis. Section 1.4 discusses about why this study is conducted, the purpose behind it and then section 1.5 describes the solution of the aforementioned goal.

CHAPTER 2

BACKGROUND

2.1 Overview

BC has a highly death rate in women and its early detection can increase the survival rate. For detection different screening techniques are being used to detect cancer at an earlier stage. Women of age 40 or above must go for screening to diagnose if they are suffering with BC. Various imaging techniques have been proposed for early detection of BC. If a patient is diagnosed with malignancy in early screening, then biopsy is performed which is considered as a definite way for diagnosing. It's an invasive method which can lead the patient to feel a minor pain because a tissue is removed from the breast for the further diagnosis of it in lab under the microscope. With the passage of time diagnosis procedures keep on improving. Now CAD models are being used for BC diagnosis which are considered as second opinion to check the decision of pathologist. As reading a histopathology image is a complex task and time consuming so with the advent of ML and DL a lot of work is being done to improve the CADs performance to better assist the radiologist. This cutting-edge technology allows for more individualized and nuanced diagnosis in addition to increasing accuracy.

2.2 Breast Cancer

In U.S, BC is the second most common leading cancer in women. To prevent, diagnose and treat the BC different researches are being done by the researchers all over the globe. It is a type of cancer which begins in cells of breast. Both males and females can be diagnosed with this disease, but most commonly females are diagnosed with this type of cancer. Irregular growth of cells in the breast forms a mass or lump which is basically called tumor. It usually develops when cells do either proliferate beyond the natural limits or they fail to die when they should ought to. This tumor can be categorized in two types. Depending on important factors likewise size, perimeter, density, gradient, and texture, a tumor may be malignant (cancerous) or benign (non-cancerous) [5].

Benign tumors are often regarded as harmless when discovered in breast tissue since they are generally "innocent," slow-growing, localized, and do not spread to other regions of the body. A malignant tumor is another word for cancer: a lesion that can migrate to distant locations and eventually can cause death (metastasize) or infiltrate and destroy nearby structures (locally invasive) [6]. It is more dangerous because it can migrate to other regions of the body, develops more quickly, and invades nearby tissues.

BC is highly deadly and prevalent. With 12% of newly diagnosed cases per year, BC accounted for the most frequent cancer form worldwide as of 2021. 15% of those cases include women who have been diagnosed with BC and have a family member who also has the disease. 85% of them have no family history. Approximately 1 in 8 women and 1 in 833 men in the United States may get invasive BC at some point in their lives. Of all malignancies, BC has the second-highest mortality rate among females in the United States [4]. As anticipated by the (WHO), 19.3 million instances of BC would be diagnosed worldwide in 2025.

After lungs cancer, it's second common and deadly cancer relates to women in the high developed nations, and causes high deaths than any of the other disease. Early detection of BC improve treatment outcomes [13]. Because early-stage tumors are frequently more localized, less aggressive treatments, targeted medications, and surgical procedures may be more effective in treating them. Survival rate can be increased by early detection and this will reduces the death rate which is crucial, but if detected early enough, 95% of instances of BC are curable [12].

2.3 Evolution of BC from Ancient Beliefs to Modern Breakthroughs

Cancer is as ancient as humanity [9], In ancient Egypt, there were the first documented reports of BC. The Edwin papyrus, which may date back to 2500–3000 BCE, describes how to cure BCs with “fire drill” which is a tool that is used for burning the skin to eliminate the diseased tissue in a number of situations when the tumors were developing in the breast [2]. At the time, the illness was thought to be incurable.

Hippocrates who is known as “Father of Medicine” [1] was the first who used the term "cancer" about 400 BCE, and according to his explanation it was caused by an imbalance of the body's humors, which include black bile, blood, yellow bile, and phlegm [2]. This was a pioneering effort to comprehend the illness. There was a thought in the past that menopause may cause cancer, this is considered because cancer is more likely to grow as one ages [2]. This viewpoint, meanwhile, was predicated on a metered understanding of medicine at the time. In 1680, Francois put out an alternative theory, speculating that cancer may have resulted from the body's lymphatic fluids becoming acidic [14].

Gendron expanded on lymphatic hypothesis by stating that the mixing of lymph with nerve and glandular tissue might result in cancer [14]. During this time, a number of ideas that attempted to explain the causes of BC emerged, which was indicative of the medical community's continuous search for answers. Ramazzini proposed the fascinating theory that nuns' contributed to an increased incidence of BC in 1713 [14]. Although it may sound unconventional, the theory that hormonal changes during pregnancy, delivery, and nursing might actually protect against BCs is supported by current research [15].

An Italian physician, used a different tack and claimed that curdled milk in the breast was the cause of BC [14]. This hypothesis illustrates the range of opinions in the historical knowledge of the origin of BC and was developed by the analysis of hundreds of patient autopsy[1] [14]. Johannes postulated an alternative theory in which pus-filled inflammations might result in BC. These theories show the variety of conjectures that have been made about BC throughout history.

[1] A post-mortem exam is performed to determine the severity of the illness or the reason of death.

A psychological component was added to the discussion by a French surgeon by claiming that depression-related mental illnesses could be a factor in BC. This psychological viewpoint also emerged in the 18th century, at the time when surgeons such as Claude-Nicolas started to explore surgical treatments for BC [14]. These operations, which include the cutting of the breast, lymph nodes, and muscles, were reflective of the 1750s knowledge of the condition and attempts to treat it [16]. To treat BC this signaled the shift in the medical community's approach from theoretical concepts to aggressive strategies.

By creating the radical mastectomy in 1894, In late 19th William Halsted made a substantial contribution to the treatment of BC. His treatment not just removes breast, but it do also removes underlying lymph nodes and muscles [17]. Although continues progress remained continued in medicine advances. Sir Astley Paston an English surgeon and anatomist, bring awareness to breast illness through his many writings on a variety of organs including breast [18]. In addition to operating on and studying thin slices of breast tissue, American surgeon Dr. Max Cutler and British surgeon Sir George Lenthal recorded their results for future generations in 1931 through "Tumors of the Breast, Their Pathology, Symptoms, Diagnosis and Treatment", which is regarded as first modern textbook of mammary pathology [19].

The invention of simple and compound microscopes[2] opened up a new realm for the visualization of diseases with the advent of microscopy [20]. Due to reason that microscopy provides tissues magnification, it gives innovation in microtomy and tissue processing and gives pathologist's[3] an ability to find complex patterns in tissues that can describe disease. Back in 1930s, when J. Collins invented BC detection methods. He discovered needle biopsy and began utilizing the frozen sectioning method to identify BC beneath a microscope [21]. This method is still using today as a straightforward, trustworthy diagnostic tool for tumors in the breast [22]. In 1937, Sir Geoffrey Keynes also developed new treatments at the same time, such as medical radiation, specifically for tumors that persisted after surgery to save the breast [17].

In 1896 William Rontgen discovered x-rays which laid groundwork for emergence of mammogram[4] [23]. The first cases of BC which were detected by mammogram were reported by

[2] An optical device for observing tiny things, including human body tissues or cells.
[3] A medical professional who does body and tissue examinations.
[4] An image of the breast obtained by X-ray. Mammograms are used by doctors to detect early indications of BC.

Robert Egan in 1962. He gave evidence that how mammograms are efficient in diagnosing and finding breast tumors and undiagnosed malignancies. BC surgery has improved because of this imaging technique, which made it possible to identify tiny BCs early on [24]. The broad use of mammography as a screening method in the 1960s was greatly aided by Egan's research [2].

The discovery of progesterone and estrogen receptors in breast tumors by Elwood Jensen in 1967 set the stage for revolutionary discoveries in the field of BC therapy [22]. With time BC operations moved toward less invasive procedures and In 1973 Holmström published the transverse rectus abdominis myocutaneous (TRAM) flap surgery, and he went on to create novel methods for breast reconstruction [25]. The National Surgical Adjuvant Breast and Bowel Project, published in 1989 by Bernard Fisher, marked the completion of the historical trend. This groundbreaking scientific study demonstrated the effectiveness of a comprehensive strategy that combines radiation, chemotherapy, and surgery in prolonging the lives of patients with BC, including those with advanced tumors.

The development of mammography in the middle of the 20th century marked a turning point in the diagnosis of BC. With the advent of mammography as a common screening method, medical practitioners could now detect anomalies and changes in structure in breast tissue. The transition from manual to imaging-based methods represented a significant development in BC early detection. The late 20th century witnessed the introduction of computerized methods for BC diagnostics as a result of ongoing technological advancements. Systems such as CAD were developed to help radiologists analyze mammograms. These technologies added an additional level of examination by using algorithms to examine photos and identify regions that could be problematic. The integration of medical knowledge and technology represented a paradigm shift in the enhancement of BC detection efficacy and precision.

The introduction of ML into the detection of BC in the 21st century marked a paradigm change. Mammography interpretation was improved with the use of ML algorithms, which have the capacity to learn from large datasets. The accuracy of early cancer diagnosis was greatly increased by ML capacity to identify patterns and abnormalities in imaging data. In this era, human expertise and computational skills have a beneficial interaction.

The combination of DL and artificial AI has advanced BC diagnosis to unprecedented levels in recent years. Highly accurate analysis of BC is made possible by DL, especially Convolutional Neural Networks (CNNs), which are excellent at picture identification and feature extraction. This cutting-edge technology allows for more individualized and nuanced diagnosis in addition to increasing accuracy.

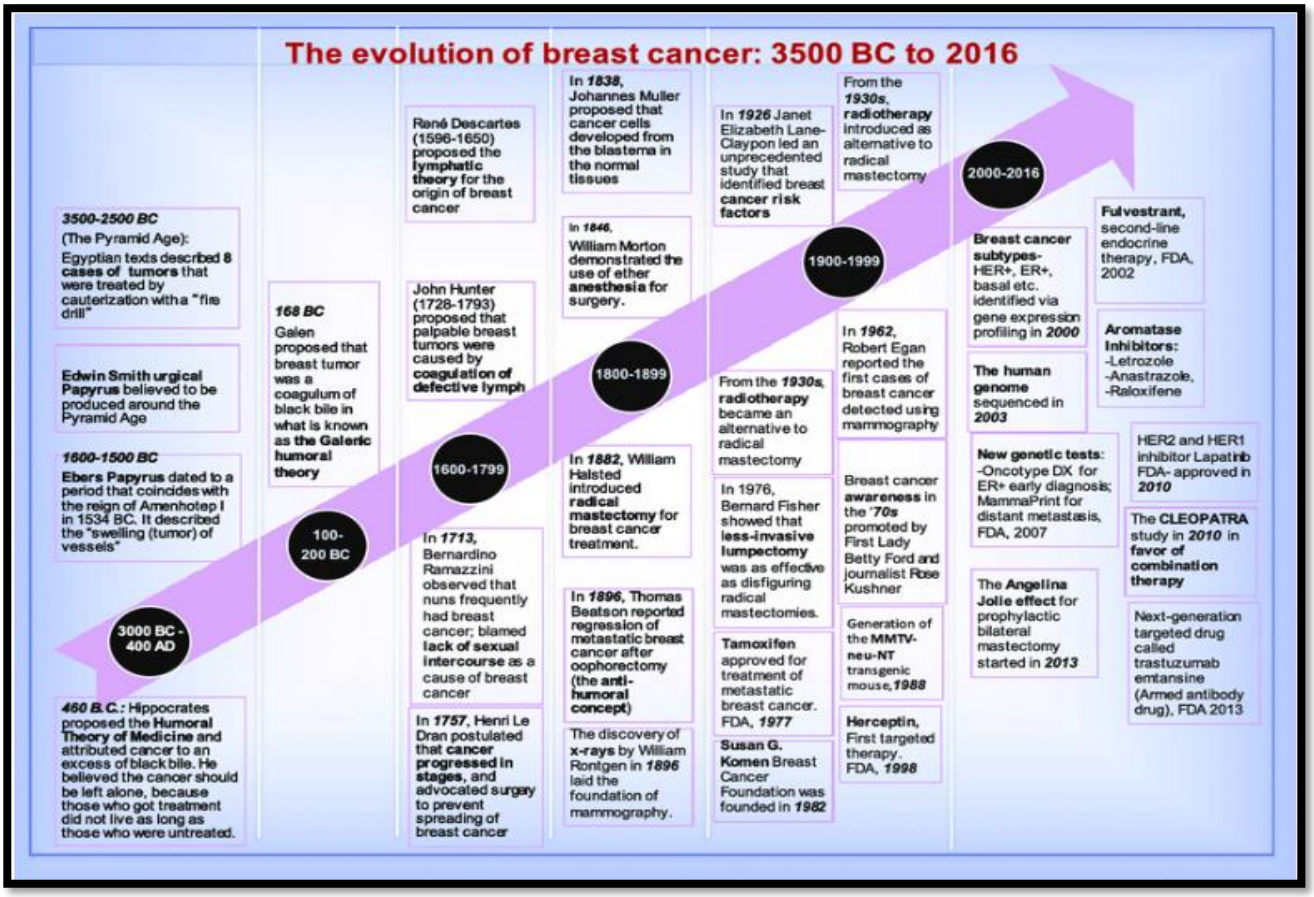

Fig 2.1: Evolution of Breast cancer

2.4 Diagnostic Techniques:

Advances in diagnostic methods occurred over the 19th and 20th centuries. Furthermore, a variety of methods and examinations including Mammography, Ultrasound, MRI, and Biopsy are currently employed in the diagnosis of BC.

2.4.1 Mammography:

Mammography, which was developed in the middle of the 20th century, was a major advancement as it made it possible to see within the breast tissues and identify anomalies [9]. An x-ray test called a mammography is done to look at the breasts. It helps to identify and diagnose breast illness in individuals with and without breast complaints, including those who have breast issues such as a lump, discomfort, or nipple discharge [26]. It makes it possible to find cysts, benign tumors, and breast malignancies before they can be felt with the hand. It is a common BC screening instrument. Mammography has been around for nearly 30 years. To get images of the interior of the breasts, a little quantity of ionizing radiation is applied to the breasts.

2.4.1.1 Mammography Procedure:

A mammography compresses the breast between two plates, allowing X-rays to penetrate the breast tissue and provide finely detailed pictures. Two perspectives of the breast are acquired. mediolateral and craniocaudal oblique. Traditional film mammography has mostly been supplanted by digital mammography.

2.4.1.2 Mammography Pros:

- A reliable and efficient screening method for identifying BC, particularly in its early stages.
- Mammography is a common for BC screening programs and is easily accessible to a wide audience.
- By identifying cancers at an earlier, mammography has helped to significantly lower the death rate from BC during the course of its decades-long usage.
- The detection of calcifications, which may be an early indicator of some forms of BC, is main specialty of mammography.

2.4.1.3 Mammography Cons:

- Ionizing radiation is exposed during mammography. Even though the danger is usually minimal, it should be taken into account, especially for periodic tests.
- Women with thick breast tissue may have less sensitive mammography results.
- For certain women, the compression of their breasts during a mammography might be uncomfortable.

2.4.2 Breast Ultrasound:

Breast ultrasonography produces images of the interior of the breasts through the use of sound waves. this technology is able to take pictures of parts of the breast that mammography could find challenging to view. Determining whether a breast lump is a solid mass or a cyst can also be aided by it [27]. It may identify small anomalies in thick breast tissue. The location of a tumor can also be determined using ultrasound, which can help a specialist do a biopsy [28].

2.4.2.1 Breast Ultrasound Procedure:

A transducer is a portable instrument that is used to travel over the skin after gel has been put to the breast. When sound waves are released by the transducer, echoes are produced that cause real-time visuals to appear on a computer screen [29].

2.4.2.2 Breast Ultrasound Pros:

- A non-invasive technique that doesn't subject the patient to ionizing radiation.
- It helps to clarify diagnosis by differentiating between solid tumors and cysts filled with fluid.

2.4.2.3 Breast Ultrasound Cons:

- Younger women with thicker breast tissue, where mammography may be less sensitive, breast ultrasonography is frequently more successful.
- In order to precisely target questionable regions during biopsy operations, breast ultrasonography is frequently utilized as guidance.

2.4.3 Breast MRI:

In order to provide detailed images of the interior of the breasts, breast MRI is a complex imaging technique that uses radio frequency pulses, a strong magnetic field, and a computer. MRI is particularly useful for women with thick breast tissue when assessing breast tumors that are not evident with mammography or ultrasound. A breast MRI may be performed to assist pinpoint the precise location and size of BC if it has already been identified [26].

2.4.3.1 Breast MRI Procedure:

The patient lays on a specially made table that slides into the MRI machine to have a breast MRI. Sometimes, to improve the visibility of certain structures, an intravenous injection of a

contrast agent usually gadolinium is used. After that, the MRI scanner takes a number of in-depth cross-sectional pictures that provide a thorough look of the breast tissue [30].

2.4.3.2 Breast MRI Pros:

- Breast MRI is so sensitive, it can find anomalies and tiny lesions that other imaging techniques would miss.
- Ionizing radiation is not used during breast MRI, which lowers the possible long-term dangers related to radiation exposure[26].
- In women with thick breast tissue, where mammography may be less sensitive, breast MRI is very helpful.

2.4.3.3 Breast MRI Cons:

- Despite being extremely sensitive, false-positive results from breast MRIs might result in further needless testing and even worry.
- In general, breast MRI costs higher than other imaging techniques.
- The often used contrast substance, gadolinium, carries concerns for people with allergies or renal issues.

2.4.4 Biopsy:

The only method that can be used to diagnose BC with precision is a biopsy. A tiny sample of breast tissue is removed during this invasive[5] treatment in order to examine it under a microscope, and evaluate whether or not a suspicious region in the breast is malignant (cancerous) or benign [31]. This inspection under microscope and biological tissues and cells study is referred as Histopathology. Images from a breast biopsy are sometimes referred to as "pathology slides" or "histopathology slides. A breast biopsy may be necessary if the patient's symptoms or the findings of an imaging test indicate that they may have BC. Additionally, it may be applied to look into unusual results from a breast exam, ultrasound, or mammography. histopathology[6] image diagnosis is gold standard for diagnosing practically all forms of cancer, including BC. The pathology reports[7] of breast biopsies can assist the physician in determining if the patient need more surgery or additional medical treatment [32].

[5] Any technique where a needle, tube, gadget, or scope is "invaded" into the body is considered invasive.
[6] Diagnosis as well as study of tissue diseases, which entails microscopic examination of tissues and/or cells.
[7] Medical report regarding an organ, tissue, or blood sample that was extracted from body.

2.4.4.1 Biopsy Procedure:

The process involves taking a sample of breast tissue so that it may be tested. During a biopsy, the physician removes a core of tissue from the doubtful location using a specialized needle instrument that is guided by an X-ray or another imaging test. Biopsy samples are submitted to a laboratory for processing. There, pathologists—doctor specialists in the study of blood and body tissue—examine the tissue samples. That samples are fixed to a glass microscope slide for microscopic inspection and staining. and determine if the cells are malignant or not.

2.4.4.2 Types of Biopsy Procedure:

These are the several forms of breast biopsy techniques, each having a unique methodology:

Fine Needle Aspiration (FNA): To remove a little sample of cells from the doubtful location, a hollow, thin needle is inserted. FNA is frequently performed to assess cysts containing fluid or to collect a sample to be used for further testing [33]. The primary drawback of FNA is its incapacity to distinguish between some benign and borderline breast tumors and malignant lesions [34].

Core Needle Biopsy (CNB): From the suspicious region, a tiny cylinder of tissue (called a core) is removed using a bigger, hollow needle. A CNB is frequently used to take a larger tissue sample for a more thorough analysis [33]. Fine needle aspiration has mostly been replaced with core needle biopsy.

Stereotactic Biopsy: With this technique, the biopsy needle is accurately guided to the doubtful spot using mammography. Stereotactic biopsy is frequently performed for microcalcifications and is utilized when the change is not readily felt or apparent.

Ultrasound-Guided Biopsy: Biopsy needle is guided to the desired location using ultrasound imaging. When the doubtful region appears on ultrasonography but is difficult to feel, this procedure is quite helpful. The acquired image is provided to pathologists for manual interpretation based on his experience.

2.5 Challenges and Limitations in terms of efficiency and accuracy:

BC is still a major worldwide health problem, and effective treatment depends heavily on early detection. Histopathology, which involves examining tissue samples under a microscope to detect if tissues are healthy or not, is an essential diagnostic technique. When analyzing these complex microscopic pictures, human eyes might occasionally overlook minor details or make mistakes. Pathologists must manually interpret histopathology pictures based on their experience to diagnose cancer, the diagnosis procedure is laborious and requires specialized knowledge. Research has demonstrated that pathologists' interpretation of histopathology pictures can result in false-positive instances.

However, patients may reach an irreversible stage due to the inherent subjectivity and possibility of human mistake in the interpretation of histopathological pictures. A double reading approach involving many pathologists is essential to improve accuracy, but it also adds to their burden because they must review a large number of photos every day, which might wear them out. The development and integration of CAD systems have resulted from this.

2.6 Computer-Aided Diagnosis:

CAD is a technology having the use of modern computer techniques, ML, and artificial intelligence, that helps medical practitioners analyze medical images. The CAD model, which can be used as a semi-automated or automatic tool, analyzes medical imaging data by applying multidisciplinary knowledge and ML techniques. At several phases of patient care, such as lesion identification, characterization, disease risk prediction, cancer staging, treatment planning, response evaluation, recurrence, and prognosis prediction, it provides findings to doctors as decision support [35].

It is a pattern recognition software, marks alarming irregularities on pictures so radiologists can see them. The CAD system helps pathologists and reduces human mistake by acting as a second opinion or double-checking method. Because biological pictures are so complex, the classification of images is a recurring problem in the area. In order to solve these issues, CAD techniques are essential in the interpretation of biological pictures. They are a useful addition that lowers the possibility of incorrect diagnoses and false-positive or false-negative outcomes, especially when it comes to the detection and classification of cancer.

Subtle patterns and anomalies in histopathology pictures that pathologists might miss are detectable by CAD systems. This improves the overall precision of the diagnosis. The objective results of CAD's quantitative analysis greatly improve diagnosis accuracy and assist less experienced doctors. Furthermore, pathologists frequently run out of time while reviewing a significant number of histopathological photos. CAD speeds up the diagnostic procedure, enabling earlier assessments and actions. CAD is a useful tool for dual reading or as a second viewpoint. Pathologists can reduce the possibility of diagnostic mistakes by validating their interpretations and cross-referencing results with the CAD system. CAD systems provide uniformity in the analysis of images, guaranteeing that every image is assessed according to defined standards. As a result, diagnoses are less variable and the outcomes are more trustworthy. In 1998, the first commercial CAD system was authorized as a second opinion by the Food and Drug Administration (FDA) [35].

When it comes to diagnosing BC from histopathology photos, CAD becomes an indispensable tool in tackling the problems caused by human subjectivity and growing workloads. Its importance in enhancing overall medical results is highlighted by its capacity to improve accuracy, deliver rapid analysis, and provide quantitative data assistance. A potential development in the fields of cancer diagnostics and medical imaging is the use of CAD for histopathology image analysis. Its analyzed that without CAD detection sensitivity is almost 80% while this sensitivity goes to 90% with CAD. Different CAD systems are being proposed in literature for both cancer detection and classification. ML based CAD models have become popular with digital microscopy development and advancement.

2.7 CAD using histopathology images for BC diagnosis:

In order to enhance analytical and prognostic capacities, computer-assisted image analysis of histopathological pictures is a potential approach. This might help histopathologists by offering a trustworthy second opinion for consistent interpretation. Important CAD system components that can help the pathologists listed below [36].

2.7.1 Step 1 Preprocessing:

In image analysis, the preprocessing stage is essential because it guarantees that the input pictures are refined, consistent, and free of unwanted changes or artifacts. Due to several factors such as distinct laboratories, uneven tissue slice circumstances, or varying imaging equipment, histopathological pictures can frequently display discrepancies in contrast, color, and staining processes. To ensure consistency throughout the dataset and standardize these variances, preprocessing is crucial.

The total image quality must be adjusted since it has a big influence on other steps like feature extraction, classification, and image segmentation. Preprocessing methods include color normalization to correct for differences in staining methods, noise reduction to preserve structural clarity, enhancement to maximize contrast, and artifact removing to highlight real tissue properties. Pixel normalization guarantees numerical stability, dataset augmentation expands the variety of training data, and image resizing helps reduce the amount of computer resources used. In order to prepare pictures for precise and trustworthy analysis in later stages of the image processing pipeline, these pretreatment processes must be carried out effectively.

2.7.2 Step 2 Segmentation:

In CAD, the main objective of segmentation is to locate and isolate particular regions within histopathological pictures that could have abnormalities or lesions in order to diagnose BC. This might entail finding other structures of interest, isolating possible tumor locations, or differentiating between various types of tissue. Precise segmentation of regions of interest is necessary for later stages of the cancer diagnostic process, which help CAD system to concentrate on areas that are likely to contain crucial information regarding possible malignant tumors.

2.7.3 Step 3 Feature Extraction:

One significant element that has a direct impact on classification is feature extraction. Finding and measuring pertinent data or characteristics inside segmented areas of histopathology images is its main objective. The majority of systems use wavelet bases, textures, statistical characteristics, spatial domain, fractal domain, and statistical qualities to characterize tissues in order to identify anomalies and categorize them as benign or malignant. This stage is essential for catching subtle details in the pictures. To extract characteristics at the cellular level, the specific

positions of the cells must be known before. Scientists invest a great deal of effort in trying to identify a set of features that will help them distinguish between malignant and normal cells more accurately. ML models use these properties or features as input data to further classify. The features used are generally determined by the particular objectives of the classification task as well as the specifics of the data.

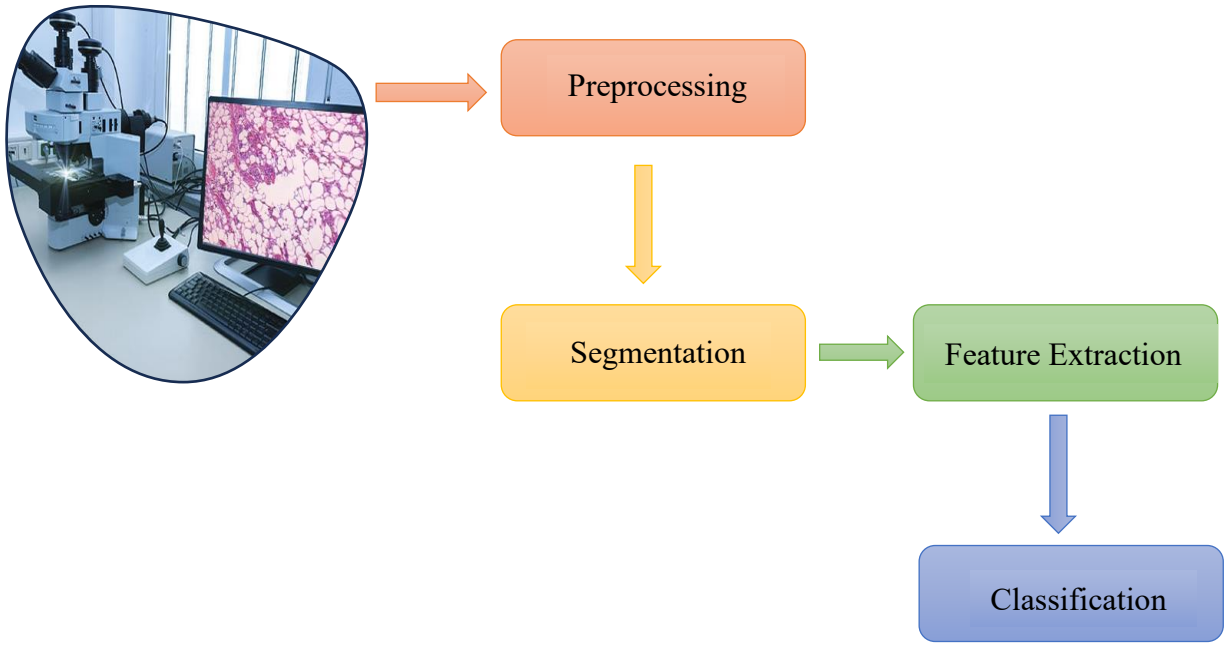

Fig 2.2: CAD System components

2.7.4 Step 4 Classification:

This stage determines, based on the training dataset, in which class the new instance falls. Various classifiers have been presented in the literature to diagnose any questionable region in the picture. Images can be categorized into subtypes or as benign or malignant depending on the particular tissue or locations. While some classifiers are just used to pinpoint suspicious areas, others are employed to categorize or determine from which class does the cell or tissues belongs. ML-based SVM, KNN, logistic regression, random forest, etc. are some of the methods used for classification; DL-based DCNNs, such as ResNet and DenseNet, can be used to classify depending on which class does histopathology image belongs.

2.8 Summary:

In this chapter section 2.2 describes about BC, its types and world widely stats. Moving forward section 2.3 discusses the era of BC from ancient times to this modern time, how its diagnosis and treatment evolved with time. Section 2.4 discusses about different diagnosing and imaging techniques their pros and cons. Section 2.5 tells about challenges in terms of accuracy and how manual reading of imaging files is difficult so in section 2.5 CAD is covered which is used for automatic classification of BC.

CHAPTER 3

Literature Review

3.1 Overview:

Beginning in the late 1950s and continuing into the late 1960s, CV gained popularity as a result of researchers' desire to educate computers "to be.,.human" . The late 20th century witnessed the introduction of computerized methods for BC diagnostics as a result of ongoing technological advancements. Using image processing techniques to analyze histopathology pictures entails a number of processes, including color normalization, feature extraction, segmentation, and classification [37]. The introduction of DL into the detection of BC in the 21st century marked a paradigm change. Especially CNNs, which are excellent at picture identification and feature extraction. This cutting-edge technology allows for more individualized and nuanced diagnosis in addition to increasing accuracy. Researchers have proposed many models for BC detection using conventional methods as well as DL based methods to improve classification results for both binary and multi-class. These models are being proposed to help pathologists as a second opinion tool for reducing the rate of misinterpretation. The goal of CAD systems is to minimize false positives and false negatives.

3.2 Comparison of Conventional Computer Vision and Deep Learning:

A comparison between the DL technique and conventional CV was presented by O'Mahony et al. in [38]. Wherein the writers explain how DL has enhanced the functionality of the conventional CV. Because DL models can automatically extract complex and sophisticated features from images, they have made significant advances in CV, particularly in biomedical image processing. This has led to the use of these models by a number of researchers to classify images related to BC histopathology.

It wasn't until Yann LeCun et.al build LeNet in the 1990s that the popularity of DL took off. The design and operation of the neural networks in the human brain served as inspiration for DL. It's a branch of ML that works with numerous neural network layers to do various imaging tasks. Convolutional Neural Networks (CNNs), in particular, are a type of DL technology that learns hierarchical features directly from raw data. CNNs gradually pick up high-level features and representations while automatically picking up low-level elements like edges and textures. Additional benefit is the neural networks can be used with other datasets as they are retrainable.

The latest advancements in CNN have greatly influenced CV and have led to a notable rise in object recognition performance. In order to classify images using conventional CV algorithms, feature extraction is necessary. Choosing which features[8] to search for in each individual image presents a challenge when using this feature extraction method for image classification. When the number of classes trying to classify starts to rise beyond, say, 10 or 20, this becomes tedious and nearly impossible.

Moreover, conventional CV approaches are less adaptable, using a different dataset requires more effort from the engineers. Assume, for instance, that a model that effectively categorizes photos as a handwritten "6" or "9" has to be modified such that the algorithm can identify photographs as either "cow" or "goat." To determine what features to employ in this adaption, an engineer would need to execute feature analysis on the cow and goat photos using a standard

[8] A feature is a portion of an image that is considered "interesting" and aids in identifying various areas within the image.

algorithm. In order to extract these features, the software would then need to be modified. The model might be retrained by replacing the dataset with one using a DL method. For the engineer, there would be no further procedures such as feature analysis. Feature analysis gets more laborious as more classes are involved, which complicates the development of classical algorithms.

End-to-end learning, which essentially instructs the machine what to look for in relation to each distinct class of object, was made possible by DL. It determines each object's most noteworthy and descriptive features. Stated differently, the task assigned to neural networks is to identify the underlying patterns within image classes. Thus, it may eliminate the need to manually select which conventional CV algorithms to apply in order to characterize your features while using end-to-end learning.

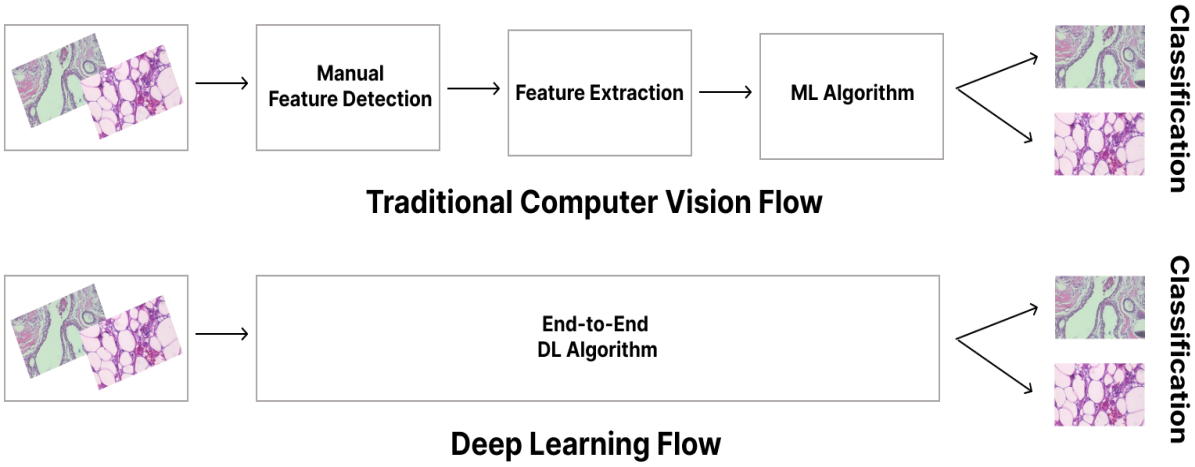

Fig 3.1: Deep Learning and Computer Vision workflow

3.3 Exploring Conventional techniques for Breast Cancer classification:

Using image processing techniques to analyze histopathology pictures entails a number of processes, including color normalization, feature extraction, segmentation, and classification [37]. In the conventional approach, as a pre-processing phase, the color normalization procedure is utilized to eliminate color and illumination variations. An extensive normalizing approach is provided in [39] to solve the issue of color variance in histopathology pictures. This work suggests saturation weighted statistics, which produce trustworthy color signals for stain-normalization. Their technique

pinpoints the reasons behind color variation. To deal with inconsistencies of histology slides which are due to intensity variations and stain, Macenko et al. [40] proposed an algorithm which improves identification of stain vector, intensity normalization for tissues better discrimination. For stain normalization, a hybrid method including two steps—stain separation and color transfer—has been devised in [41]. A color transfer algorithm is utilized to reduce the impact of changing staining and light and A weighting factor was added in order to modify the normalized image's brightness and contrast.

Following color normalization, the most discriminative features are retrieved using feature descriptors, and an ML algorithm is then trained for classifying the photos into several groups according to the features that were extracted. Conventional CV techniques frequently depend on manually created features and basic ML models. The difficulty of feature extraction increases with the number of classes that need to be classified. During a protracted process of trial and error, the CV engineer must use judgment to identify which features best characterize which class of objects. Additionally, each feature description requires the CV engineer to handle a multitude of parameters, all of which must be adjusted. Features like edge detectors, texture features, statistical features, and color features can be extracted for the purpose of classification[9] of images [37].

Hand-crafted features were extracted by Butler et al. [42] that uses Naive Bayes (NB) classifiers along with features selection to find BC, and reached 90% of accuracy and used X-Ray scatter images. Street et al. developed ML based model in 1993. To address the problem of BC categorization ensemble learning in conjunction with textural and statistical features was presented in [43]. It combined statistical features extractors like Haralick, which disclosed 24 features, with texture features extractors like SIFT, ORB, and SURF, each of which revealed 256 features, to create a potent ensemble model. These features were then deftly merged using a stacking approach, in which the data is analyzed by many ML models (XGBoost, Random Forest, etc.), and the predictions are then mixed. Using CatBoost classifiers and stacking, this method achieved an astounding 92.55% accuracy in categorizing IDC(+) and IDC(-) pictures, outperforming individual

[9] The process of classification involves giving labels to various groups according to the features that have been recognized.

feature categories. Through the identification and removal of duplicate characteristics, the study creates a lightweight, computationally efficient, model.

To find suspicious regions Liu et al. [44] offered a method that takes into account an adaptive region-growing technique. Regions of interest (ROIs) were then classified by using the geometrical and texture features extracted by the Gray-Level Co-occurrence Matrix (GLCM) and completed local binary pattern (CLBP). Support vector machines (SVMs) were used to classify the ROIs. The most straightforward and economical method was suggested by Sethy et al. [45] Mammography pictures with the abnormalities were scanned using the SVM classifier and HOG features, indicating the BC. In addition to the detection, precise pinpoint location of the breast anomaly can also be detected.

Kowal et. al focused on nuclei segmentation in [46]. To categorize the breast histology pictures, a collection of features was retrieved and put into conventional classifiers such k-NN, naive Bayes, and decision trees once the region of interest was chosen. Study was done on tiny data sets of 500 pictures from 50 patients. Reis et al. looked at an automated system to categorize stromal areas based on their maturity in [47]. LBP and basic image features were retrieved at many scales. The stromal areas were classified using a random decision tree classifier. The study employed 55 invasive BC pictures that were stained with Hematoxylin and Eosin. An 84% classification accuracy was recorded.

In [48], Zhang et al. incorporated LBP, statistics from GLCM, and curvelet transform, utilizing a cascade random subspace ensembles technique with reject choices. This work also focused on obtaining global, shape, or local features from the pictures. The authors attempted to resolve the simple instances at the first level of the cascade, and in subsequent levels, they submitted the difficult cases to a more intricate pattern classification system. Six classifiers were used to classify the samples into three categories: normal tissue, carcinoma in situ, and invasive cancer, with a maximum accuracy of 99.25%.

To aid in the creation of CAD systems, a method based on the relationship between curvelet transform, local binary patterns (LBP), feature selection by statistical analysis, and unique classification technique was introduced by Bruno et al. in [49]. The photos were processed to extract LBP and curvelet features. The statistical analysis of variance (ANOVA) eliminated the

related features. Decision trees, random forests, SVMs, and polynomials (PL) were employed in the classification process. Higher accuracy was attained between 91% and 100% when the PL classifier was associated with the curvelet transform, LBP, and ANOVA.

Using color normalization as pre-processing, Scale Invariant Feature Transform (SIFT) and Discrete Cosine Transform (DCT) features with an SVM for classification, Mhala et al. [50] have categorized a set of histopathological pictures. The approach reports 98.88% accuracy for invasive carcinoma class and 100% accuracy for both ductal carcinoma in-situ and normal class pictures. True et al. [51] presented the first use of image processing in analytical pathology for cancer identification, demonstrating the significance of morphological aspects in malignant tumor diagnostic techniques. To find cell anomalies, they employed a number of morphological features, such as area fraction, shape, size, and item counting.

R. et. al in [52] proposed a two-stage categorization system for BC. K-Means clustering was used to segment the nuclei, moreover features were extracted using the Discrete Wavelet Transform (DWT) technique. Using SVM, classification accuracy was attained at 93.3% on BreaKHis dataset. The study in [53] includes classification, image data analysis, and raw data pre-processing. Contrast-limited adaptive histogram equalization and Gaussian filtering was applied for picture enhancement. In order to separate nuclei for later integrated feature extraction, segmentation used k-means clustering. By integrating geometrical, color, and texture information with SVM as the classifier, achieved 90% test accuracy on the UCSB and BreaKHis datasets.

Despite significant advancements, these techniques still have a number of glaring drawbacks. They first demand a significant time and labor investment. They made the majority of the features by hand. Secondly, the conventional models have limited sample sizes and are unable to perform end-to-end training, leading to sub-optimal results. The CAD models' applicability is somewhat restricted by all of them.

3.4 Exploring Deep Learning techniques for BC classification:

We are currently living in the age of DL. In order to perform associated CV tasks such as target identification and classification, CNNs have been employed extensively. An increasing

number of researchers are using CNN to do pathological image classification, motivated by excellent publications.

Using transfer learning and generative adversarial networks (GANs), a DL-based method for classifying BC was presented by Thuy et al. [54] the architecture classify the features retrieved from histopathology pictures after fine-tuning the VGG16 and VGG19 networks to extract features. GANs were used to produce more training data. And model had an average accuracy of 95.0%. The computational cost of the suggested method and the fact that the GANs utilized in the study do not produce images that are exactly like actual histological images are among the study's drawbacks.

For constructing attention network, Toğaçar et al. [55]used three combined blocks recursive blocks, attention blocks and dense blocks and achieved 98.80% image-level accuracy. In [56] Spanhol et al. used AlexNet for binary classification at image level and at patient level. Additionally, they provide a number of training approaches for the CNN architecture, based on the extraction of patches that are acquired at random or using a sliding window method. Using the BreaKHis dataset, the authors assessed their approach and found that, on average, their method obtained 82.4% picture level accuracy and 84.4% patient level accuracy.

The performance of fully-trained and fine-tuned pre-trained networks is compared in [57]. For fine-tuning and full-training, three pre-trained networks (VGG16, VGG19, and ResNet50) were used. The findings showed that the optimal performance was attained by the fine-tuned, pre-trained VGG16 with logistic regression classifier, which had an accuracy of 92.60%, an AUC of 95.65%, and an APS of 95.95% with 90%–10% train–test data splitting. Additionally, they discovered that pre-trained networks with fine-tuning are more resilient to training data quantity than fully-trained networks.

In [58] Nahid et al. extracted structural and statistical information from the pictures through unsupervised clustering and uses this clustered data for guiding the DNN models. Three distinct DNN models were tested: an LSTM model, a CNN-based model, and a hybrid model that included the features of both the LSTM and CNN models. And the CNN-based model performed better than the other two models. On the 40x, 100x and 400x dataset, obtains an accuracy of 90.00%, on

200x it achieves 91.00%. The study also comes to the conclusion that Softmax layers outperform SVM layers in general when it comes to classifier performance.

Nahid et al. [59] presented two novel CNN based models. For the first model, Contourlet Transform (CT) and histogram-based information are used to extract local feature information from the photos. The Discrete Fourier Transform (DFT) and Discrete Cosine Transform (DCT) are two methods used in the second model to extract frequency-domain information from the pictures. The outcomes demonstrated that the CNN-CH scenario performed the best, making use of CT and histogram-based data. Recall value: 98.20%, Specificity: 94.94%, Accuracy: 97.19%.

Saxena et al. conducted a feature extraction comparison of 10 distinct pre-trained CNNs in [60]. The original histopathology pictures were split up into non-overlapping patches, and the final image feature vector was created by combining the feature vectors of each patch. and a linear SVM classifier was trained using the features that were extracted. The pre-trained ResNet50, ResNet101, and AlexNet were determined to be the best effective feature extractors. The models' performances varied depending on the magnification, Certain classifiers performed better at lower magnifications, while others performed better at higher magnifications. With an accuracy of 93.99%, ResNet50_SVM achieves the best performance for the 40×. The maximum accuracy of ResNet101_SVM was 94.81% at 100X magnification. The maximum accuracy of ResNet50_SVM was 95.91% at 200X magnification. At 400X magnification, AlexNet_SVM's accuracy was the greatest at 89.48%. For both benign and malignant instances, the ResNet50_SVM, ResNet101_SVM, and AlexNet_SVM models provided higher detection rates. AlexNet, VGG16, VGG19, ResNet18, ResNet50, ResNet101, Inception-v3, Inception-ResNetV2, GoogLeNet (Inception-v1), and SqueezeNet are the pre-trained CNNs used in study.

A novel CNN with 152 layers named ResHist was proposed in [61], which was inspired by ResNet50, prevents vanishing gradients and learns features at several levels of abstraction by using residual blocks and skip connections. The model yields accuracy of 84.34% and F1-score of 90.49% in the absence of data augmentation, and 92.52% accuracy and F1-score of 93.45% in the presence of data augmentation. According to the study, images with a magnification of 200x provide the greatest biased information for classifying.

NucTraL+BCF, a unique framework utilized in [62], is composed of nucleus guided transfer learning and belief theory based classifier fusion. From preprocessed histopathology images, the technique isolates non-overlapping nuclei patches, taking use of the fact that variations in nuclei structure imply malignancy. Features are then extracted from these patches using pre-trained CNNs ResNet-18, ResNet-50, ResNet-101, GoogleNet, and AlexNet. These features are then concatenated using p-norm pooling, and SVM is used as the classifier. Lastly, for improved classification, a fusion technique based on belief theory merges the outputs of several CNN-SVM combinations. With an astounding 96.91% accuracy rate, 97.24% sensitivity, and 96.18% specificity, NucTraL+BCF performs well. Using 60 nucleus patches and a testing duration was 4.5 seconds each picture.

Al-Haija et. al shown in [63], The CNN model makes use of transfer learning, in which the ResNet-50 pre trained on ImageNet weights, fine-tuned for the BreaKHis dataset. It enables effective feature extraction and 99% accuracy in classification. Karthik et al. [64] demonstrated how effectively channel and spatial attention can be integrated with DL approaches to improve BC categorization. They suggested utilizing DAMCNN and CSAResnet in an ensemble learning method. For enhanced feature extraction, CSAResnet combines a spatial attention (CSA) module and an additional channel with a pre-trained Resnet-101 model. Conversely, DAMCNN leverages the CSA module in Densenet-201 for better feature representation, combining the advantages of the Densenet-201 and Efficientnet-B0 models. To overcome the imbalance in classes, data augmentation was implemented. With the suggested ensemble method, an astounding 99.55% accuracy was attained.

DenTnet, which uses DenseNet as its foundation and harnesses the potential of transfer learning, was proposed by Wakili et al. [65] Four distinct components make up its architecture: input volume, transfer learning, training from scratch, and fusion and recognition. While the "transfer learning" block used the previously trained DenseNet model for feature extraction, the "training from scratch" block extracts features directly from the input pictures. Lastly, these characteristics are combined in the "fusion and recognition" block, for classification a fully connected layer with SoftMax activation used. The model attains an impressive 99.28% accuracy rate. It also yields remarkable results with an AUC of 0.99, sensitivity of 97.73%, and specificity

of 100%. They also look at the ideal ratios for training and testing, and the results show that an 80%:20% ratio produces the best results.

For utilizing high resolution images into model without compression this study [66] offered an approach by merging a Fully Convolutional Network (FCN) for high-level feature extraction with a Bi-directional Long Short-Term Memory (Bi-LSTM) to examine temporal dependencies of features. Regardless of the size of the input image, the FCN functions work as an encoder to extract key features from it. The flatten layer then turns the extracted features into a 1D vector and given to the Bi-LSTM network, to examine the temporal dependencies. At 200x magnification, the proposed FCN-Bi-LSTM model reached an average accuracy of 96.32%, which was much greater than the pre-trained AlexNet model.

In [67] authors presented twenty-eight hybrid architectures that combine four classifiers (MLP, SVM, DT, and KNN) for a binary classification over the BreaKHis and FNAC datasets with seven DL techniques (DenseNet 201, Inception V3, Inception ReseNet V2, MobileNet V2, ResNet 50, VGG16, and VGG19) for feature extraction. With accuracy values achieving 99% for the FNAC dataset, and 92.61%, 92%, 93.93%, and 91.73% for the four magnification factor values 40X, 100X, 200X, and 400X, respectively of the BreaKHis dataset, the hybrid architecture using the MLP classifier and DenseNet 201 for feature extraction (MDEN) was the best performing architecture.

To extract just nucleus structure, George et al. [68] utilized pre-trained CNNs like AlexNet, ResNet-18, and ResNet-50 for feature extraction from individual nuclei patches. After being extracted, these features are combined and supplied to an SVM (support vector machine) for classification and classification results are merged through belief theory-based fusion technique. This approach produced an astounding 96.88% accuracy, 97.30% sensitivity, and 95.97% specificity and AUC of 0.9942.

An embedded fusion mutual learning (EFML) approach was presented in this study [69] to address complementary knowledge amongst heterogeneous networks. For feature extractors, mutual learning between two heterogeneous networks is performed. In order to learn from feature maps and logits output concurrently, a feature fusion classifier and ensemble classifier are incorporated into EFML. Three datasets were utilized to assess the generalization capacity of

EFML. On the BreaKHis dataset, accuracy was 97.36%; on the BACH dataset accuracy was 98.96%; and on the LC25000 dataset accuracy was 100%.

To examine ensemble learning and transfer learning in [70] a hybrid architecture employing three feature extractors (DenseNet_201, MobileNet_V2, Inception_V3) with boosting algorithms (ADB, GBM, LGBM, XGB) as classifiers and Decision Tree as a base learner was presented. The optimal boosting ensemble, which was built with 200 trees, Inception_V3 as the feature extractor (FE) using XGB, has an accuracy rating of 92.52%. Using inception and residual block, Singh et al. design a two-stage training method in [71]. While residual blocks collect residual features via batch normalization and pre-activation, inception blocks use different kernel sizes to extract multilevel features. Extracted feature maps from both blocks are input into a sigmoid function after being concatenated and flattened. And the highest accuracy of 86% was attained on the 200X on the BreaKHis dataset, and 85% on the BHI dataset.

The pre-trained CNN is used by the authors in [72] to extract local characteristics, which are further improved by their Fisher Vector (FC) encoding and adaption layer and employed the SVM classifier. Their model obtained 87% accuracy on the image level and 90% accuracy on the patient level.

The first study on an automatic multi-class BC classification model in the literature has been proposed by Han et al. in [73]. The authors suggest a novel class structured deep convolutional neural network (CSDCNN) method for BC multi-classification. The purpose of the CSDCNN is to categorize histopathology pictures by learning hierarchical feature representations from the images. An accuracy of 93.2% was attained on average using the suggested method. Additionally, the scientists assessed two distinct training approaches: transfer learning and training from scratch. Compared to the training from scratch technique, the transfer learning strategy produced better outcomes.

Jannesari et al. provide a DL system for classifying BC subtypes and various other cancer types using histopathology pictures in [74]. The five processes of the framework are as follows: acquiring images, augmenting data, preparing DL, fine-tuning pre-trained models through transfer learning, and classifying using Inception and ResNet networks. Tissue microarray (TMA) samples were utilized to classify cancer types, and the BreaKHis database was used to classify BC subtypes.

According to the paper's findings, ResNet frameworks perform better than Inception frameworks. With ResNet50, the accuracy was 99.8% for cancer types; with ResNet152, it was 98.7% for BC types; for benign sub-types it was 94.8%; and for malignant sub-types it was 96.4%.

The IRRCNN model, which combines the advantages of the recurrent convolutional neural network, residual network, and inception network, was presented by Alom. et al [75]. The work uses two datasets BreaKHis and BCC 2015 and combines image-wise and patch-wise evaluation with data augmentation. The model achieves 97.57% and 96.84% accuracy on multi-class for image-level and patient-level, respectively using the BreaKHis dataset. Additionally, 97.57% and 97.65% of patient-level and image-level in the binary class. The testing accuracy for BCC 2015 is 97.51% for binary instances and 97.11% for multi-class cases.

Two modules based RANet-ADSVM [76] was proposed by Y. Zhou et al. RANet is used for resolution-adaptive classification while ADSVM is used for anomaly detection. Firstly, ADSVM filters and replaces incorrectly identified patches in cancerous photos to enhance RANet's training efficiency. RANet then uses subnetworks with different resolutions and depths to classify images according on their difficulty. This adaptive technique contributes to a 50% reduction in computational cost without sacrificing accuracy. RANet-ADSVM obtains an image-level accuracy of 99.14% for binary classification and 98.05% for multiclass classification on the BreaKHis dataset. Furthermore, it attains a patient-level accuracy of 97.43% for multiclass and 98.83% for binary classification. It achieved 96.37% multiclass and 97.43% binary classification patch-level accuracies, as well as 97.75% multiclass and 99.25% binary classification image-level accuracies on the BACH 2018 dataset.

BMIC_Net in [77], a DL model is introduced by Murtaza et al. It makes use of a hierarchical technique in which a binary classifier (BC1) first classifies images as benign or malignant, after that two multiclass classifiers (B2 for benign and M2 for malignant) further classify images into specific subtypes. For effective feature extraction, BMIC_Net combines transfer learning with the pre-trained AlexNet architecture. Principal Component Analysis (PCA) and Information Gain (IG) are two feature reduction approaches that are used to choose the most informative features for better classification performance. At each level, the six classic ML algorithms—KNN, SVM, NB, DT, LDA, and LR are assessed for classification. Moreover, at all classification levels, KNN is the most effective classical ML algorithm. The first-level BC1 classifier has an accuracy of 95.48%,

whereas the malignant and benign subtypes' B2 and M2 classifiers have respective accuracy of 94.62% and 92.45%.

Using the pre-trained Inception-ResNet-v2 network on ImageNet, Ferreira et al. [78] extracted features and classified images into four groups. In first phase the newly inserted top layers undergo high learning rate training. The second stage then includes fine-tuning individual feature extraction layers with a much lower learning rate. To further avoid overfitting, dropout and global average pooling were used. 90% accuracy is a promising result for the model.

For binary classification, benign subtype classification, malignant subtype classification, and grade identification, Zewdie et al. employed ResNet-50 in [10]. Before being fed into the model, images go through preprocessing, which includes scaling, normalization, augmentation, contrast enhancement, and histogram matching. A UI that is easy to use has been created for possible medical applications. Using datasets from JUMC, BreaKHis, and Zendo, the system was trained and verified, and it demonstrated exceptional accuracy in a variety of classification tasks. According to test results, the accuracy of the suggested technique for binary classification, benign sub-type classification, malignant sub-type classification, and grade identification is 96.75%, 96.7%, 95.78%, and 93.86%, respectively.

Kumar et al. offered a more fast and computationally efficient hybrid model for multi-classification that is independent of magnification in [79]. Real-time data augmentation is used to manage memory. Features are extracted via pre-trained Xception and VGG16 models, whereby the final classification layer is replaced for eight sub-classes. A LR classifier receives the extracted characteristics after which it makes predictions. Compared to VGG16 + LR, the Xception + LR model performs better, obtaining 82.45% accuracy and a quicker training time of 36.57 minutes. The depth-wise separable convolution layers of Xception are responsible for its success.

Bardou et al. investigated two methods in [80]. The first method uses bag-of-words and locality-constrained linear coding to extract features that are manually created. After that, Support Vector Machines encrypt and train these features for classification. The second method uses DL and creates CNN specifically for the purpose. For binary class CNN achieved an accuracy between 96.15% - 98.33% and for multiclass accuracy was between 83.31% - 88.23%.

Wan et al. employed a hybrid active contour model based segmentation approach to extract nuclei from the pictures [81]. They described grading the BCHI using a cascade ensemble method. An SVM classifier was trained using CNN's extracted object, pixel, and semantic level characteristics. 106 biopsy slides were used in the investigation.

Using the whole slide images (WSI) a diagnosis framework was presented [82] which uses classification advantages along with content based image retrieval. For every super pixel a probability of malignancy was given through content based approach, and a probability map was calculated through which malignant regions can be detected using WSI images. SIFT based bag of features were presented, their method named as SIFT-BoF-CBIR.

To fine tune the learning process of CNN an optimization technique was used by Alhussan et al. [83] called Advanced Al-Biruni Earth Radius optimization algorithm. and for extracting features they leverage the pre-trained AlexNet power. To evaluate model two datasets were used and achieved an average accuracy of 97.95%. A model using Principal component Analysis (PCA) as feature extractor and Deep Neural Network (DNN) as a classifier was proposed in [84] and their model named PCA-DNN. In addition to the proposed network they also compared it with ML classifiers like AdaBoost, RF, NB, SVM, and traditional DNN. Results had shown that PCA-DNN performed better than ML and existing DNN with an accuracy of 98.83%.

A feature fusion module, a residual collaborative branch, and a transfer learning backbone branch made up collaborative transfer-network (CTransNet) [85]. To extract image characteristics from ImageNet, the transfer learning branch used the pre-trained DenseNet structure. Target features were cooperatively extracted from histopathological pictures by the residual branch. CTransNet trained and optimized using the feature fusion technique, which involves optimizing these two branches. CTransNet demonstrated a 98.29% classification accuracy in experiments.

To boost classification models a YOLO detector was used by [86]. The YOLO detector is utilized to identify breast lesions using all of the input breast photos. Next, the updated DL classifiers of the normal feedforward CNN, ResNet-50, and InceptionResNet-V2 are fed individually with the discovered breast lesions. The classifiers were able to ignore the surrounding normal tissues during this detection step and concentrate solely on learning the deep properties of the identified breast lesions. With an accuracy of 99.17% for the DDSM dataset and 97.27% for

INbreast, the integrated DL YOLO detector with the InceptionResNet-V2 classifier attained the best diagnosis performance.

Table 3.1: Comparison of ML methods design for BC diagnosis

Authors	Dataset	Extracted Features	Feature Extractors	Preprocessing	Methodology	# of Class	Accuracy
2021 Roy et al. [43]	Invasive ductal carcinoma (IDC)	Textural, Statistical features	Haralick, SIFT, ORB, SURF	-	Features merged by stacking approach. And CatBoost classifier	2	92.55%
2021 Sethy et al. [45]	MIAS	HOG	-	Histogram Equalization, CLAHE	SVM	-	99.64%
2021 Aswathy et al. [53]	UCSB BreakHis	-	GLCM	Image Enhancement using CLAHE and Gaussian filter	SVM KNN RF ANN	2	UCSB dataset: 91% BreaKHis dataset: 89.1%.
2018 R. et al. [52]	BreakHis	-	DWT	Image Enhancement	SVM	2	93.3%
2017 Reis et. al [47]	-	Multi-scale Basic Image features, LBP	-	Color Normalization	Decision Tree	2	84%
2016 Bruno et al. [49]	DDSM, UCSB, BCDR	Local Binary Patterns, Curvelet features	-	-	Decision trees, Random forests, SVMs, Polynomials	2	Between 91% and 100% using PL classifier
2016 Mhala et al. [50]	-	-	SIFT, DCT	Color Normalization	SVM	3	98.88% IC 100% for DC 100% for normal

2015 Liu et al. [44]	DDSM	Texture, Geometry features	GLCM, CLBP	-	SVM	2	82.4%
2015 Zhang et al. [87]	Dataset from Israel Institute of Technology, OCT, UCI	Local textural, Global	LBP, GLCM, Curvelet Transform	-	Kernel principal component analysis (KPCA)	-	92.06%
2013 Kowal et. al [46]	500 real case medical images	GLCM, topological feature.	-	Noise reduction, Artifacts removal	KNN, Naïve Bayes, Decision Tree	2	96-100%
2013 Zhang et al. [48]	Dataset from Israel Institute of Technology	Local textural, Global, Shape features	LBP, GLCM, Curvelet Transform	-	MLP, LR, KNN, Naïve Bayes, SVM, Fisher Linear Discrimination	2	99.25%
2003 Butler et al. [42]	X-Ray Scatter Images	Handcrafted Features	-	-	Naive Bayes	2	90%

Table 3.2: Comparison of DL methods design for BC diagnosis

Authors	Dataset	Feature Extractors	Preprocessing	Methodology	# of Class	Accuracy
2023 Li at al. [69]	BreakHis BACH LC25000	-	Augmentation	Embedded fusion mutual learning	-	BreaKHis At 100X: 97.36%; BACH: 98.96%; LC25000: 100%
2023 Alhussan et al. [83]	DDSM Dataset-2	AlexNet	Augmentation	Advanced Al-Biruni Earth Radius -CNN	2	DDSM dataset: 96.2% Dataset-2: 99.4%

2023 Liu et al. [85]	BreakHis	DenseNet, Residual branch	Augmentation	CTransNet	4	40x:98.29% 100x:97.77% 200x:96.93% 400x:96.05%
2022 Karthik et al. [64]	BreakHis BACH	-	Augmentation	Ensemble of DAMCNN and CSAResnet	-	99.55%
2022 Wakili et al. [65]	BreakHis	DenseNet	Augmentation, Stain Normalization, Intensity Normalization	DenTnet	2	99.28%
2022 Singh et al. [71]	BHI BreakHis	-	-	Hybrid network comprises inception and residual block.	2	BreakHis dataset: 40x:80.8% 100x:82.76% 200x:86.55% 400x:85.80% BHI dataset: 85%
2022 Y. Zhou et al. [76]	BreakHis, BACH 2018	-	Normalization, Patch extraction, Augmentation	RANet-DSVM	2, 4	BreakHis multiclass: Image level: 98.05% Patient level: 97.43% BreakHis binary: Image level: 99.14% Patient level: 98.83%
2022 Tummala et al. [88]	BreaKHis	-	-	Swin transformer	2, 4	Binary: 99.6% Multiclass 40x:96% 100x:92.6% 200x:93.5% 400x:93.4% All zoom factors: 93.4%
2021 Zewdie et al. [10]	BreakHis, Zendo, JUMC	-	CLAHE, Augmentation, Histogram matching	ResNet50	2, 4	Binary: 96.75%, Benign sub-type: 96.7% Malignant sub-type: 95.78% Grade: 93.86%

2021 Baccouche et al. [89]	CBIS-DDSM, INbreast, Private dataset	-	Histogram Equalization, Augmentation	YOLO	2	CBIS-DDSM dataset: 95.7% INbreast dataset: 98.1% Private dataset: 98%
2020 Thuy et al. [54]	BreaKHis	VGG16 VGG19	GANs	CNN	2	95.0%
2020 Toğaçar et al. [55]	BreaKHis	-	Augmentation	BreastNet	2	98.80%
2020 Al-Haija et al. [63]	BreakHis	-	Real-time data Augmentation	ResNet-50	2	99%
2020 Al-antari et al. [86]	DDSM, INbreast	-	Multi-threshold peripheral equalization, Adaptive Histogram equalization, Augmentation	Mass detection using YOLO. For classification: CNN, ResNet-50, InceptionResNet-V2	2	DDSM dataset: 99.17% INbreast dataset: 97.27%
2019 Alom et al. [75]	BreakHis, BCC 2015	-	Augmentation	IRRCNN	2, 4	BreakHis multi-class: Image level: 97.57% Patient level: 96.84% BreakHis binary: Image level: 97.65% Patient level: 97.57%
2019 Budak et al. [66]	BreakHis	FCN	-	Bi-LSTM	2	40x:95.69% 100x:93.61% 200x:96.32% 400x:94.29%
2018 Nahid et al. [59]	BreakHis	CT, LBP, Histogram for local-features. DFT for frequency domain.	-	CNN-CH	2	200x: 97.19%.

2018 Jannesari et al. [74]	TMA, BreakHis	-	Format conversion, Augmentation	Inception, ResNet	2, 4	Cancer types: 99.8% BC types: 98.7% Benign sub-type: 94.8% Malignant sub-type: 96.4%
2018 Ferreira et al. [78]	ICIAR 2018	-	Augmentation	Inception-ResNetV2	4	90%
2017 Han et al. [73]	BreakHis	-	Augmentation	Class structure based deep convolutional neural network (CSDCNN)	4	93.2%
2016 Spanhol et al. [56]	BreaKHis	-	-	AlexNet	2	Image level: 82.4% Patient level: 84.4%

Table 3.3: ML and DL hybrid models comparison for BC diagnosis

Authors	Dataset	Feature Extractors	Preprocessing	Methodology	# of Class	Accuracy
2023 Rani et al. [84]	WDBC	PCA	-	PCA-DNN	2	98.83%
2022 Zerouaoui et al. [67]	BreakHis FNAC	DenseNet201, Inception V3, Inception-ReseNet V2, MobileNet V2, ResNet 50, VGG16, VGG19	Intensity Normalization, CLAHE	28 hybrid architectures using four classifiers: MLP, SVM, DT, KNN	2	Using MLP and DenseNet201 FNAC dataset: 99% BreakHis dataset 40x:92.61% 100x:92% 200x:93.93% 400x:91.73%
2022 Nakach et al. [70]	BreakHis	DenseNet_201, MobileNet_V2, Inception_V3	Intensity normalization, CLAHE, Augmentation	ADB, GBM, LGBM, XGB	2	Using Inception_V3 and XGBA: 92.52%

2022 Kumar et. al [79]	BreakHis	Xception, VGG16	Real-time Augmentation	Logistic regression	4	Using Xception + LR: 82.45%
2020 George et al. [62]	BreakHis	ResNet-18, ResNet-50, ResNet-101, GoogleNet, and AlexNet	Image Sharpening, Gamma correction, Stain normalization	NucTraL+BCF framework (Nucleus patches + transfer learning + classifier fusion)	2	96.91%
2020 Saxena et al. [60]	BreakHis	AlexNet, VGG16, VGG19, ResNet18, ResNet50, ResNet101, Inception-v3, Inception-ResNetV2, Inception-v1, SqueezeNet	Non-overlapping patches	SVM	2	Using ResNet50_SVM 40x: 93.99% 200x: 95.91%, Using ResNet101_SVM 100x: 94.81%, Using AlexNet_SVM 400x: 89.48%
2020 Gour et al. [61]	BreakHis	ResHist	Augmentation: Affine transformation, Image patches, Stain normalization	KNN, SVM, RF, QDA	2	Using SVM: Without augmentation: 84.34%, With augmentation: 92.52%
2020 Murtaza et al. [77]	BreakHis	BMIC_Net	Augmentation	KNN, SVM, NB, DT, LDA, LR	2,4	BC1: 95.48%, B2: 94.62%, M2: 92.45%
2019 George et al. [68]	BreakHis	AlexNet, ResNet-18, ResNet-50	-	SVM	2	96.88%
2019 Kaur et al. [90]	Mini-MIAS	CNN	Noise reduction using Median filter	K-mean clustering + MSVM	2	Normal: 95% Benign: 94% Malignant: 98%
2018 Shallu et al. [57]	BreakHis	VGG16, VGG19, ResNet50	Augmentation	Logistic regression	2	Using VGG16 and LR classifier: 92.60%

2018 Nahid et al. [58]	BreakHis	CNN, LSTM, CNN+LSTM	-	Softmax out performs SVM.	2	40x: 90%; 100x: 90%; 200x: 91%; 400x: 90%.
2018 Song et al. [72]	BreakHis	CNN and refine features through Fisher vector (FC)	-	SVM	2	Image level: 87% Patient level: 90%

3.5 Summary:

In this chapter, a comparison between existing studies for BC classification is conducted. Different authors tried different models to come up with more robust system to automatically detect BC. Both binary and multiclass classification models were under consideration. From above studies Kaur et al. achieved the highest accuracy for a multiclass classification using MSVM for classification and CNN for feature extraction. For binary classification Al-Haija et al. achieved the highest accuracy of 99% using ResNet50. From studies it is learned that the number of epoch used to train a model are really model. To achieve highest accuracy it is required to run over many epochs but until the point where accuracy keep improving for validation.

CHAPTER 4

Methodology

4.1 Overview:

For early diagnosis of BC and to reduce mortality rate and increase survival rate, there's much need to design an automatic robust model that can be installed in Laboratories and hospital. With a purpose to design a robust classifier, a CNN based DL model is used in this study. Only diagnosing BC into benign and malignant class is just no enough for starting course of treatment, so further analysis is required. That's why a multiclass classification model is designed. Figure 4.11 presents the detailed architecture of the proposed model.

For classification of Histopathological images into benign, malignant and further subclasses the model designed in study consists of multiple modules such as Data collection, Preprocessing steps like (down sampling, splitting, resizing, augmentation, and balancing), Feature extraction and classification using the proposed solution. These steps are explained in more detail in the below sections.

4.2 Data Collection:

For designing an image classifier first step need to done is collection of data, that will be passed to the model for training so it can classify images. So publicly available dataset BreaKHis is selected and downloaded because its most reliable available dataset.

4.2.1 Dataset:

The dataset BC Histopathological Image, known as BreaKHis [6], is used in this work. Images taken from a biopsy process, in which a little sample of tissue is removed for microscopic analysis, are included in the collection. After the biopsy, the tissue samples are submitted to a lab where they are examined and analyzed in-depth under a microscope by a pathologist. The examination of biological cells and tissues under a microscope is referred to as histopathology. The Greek word "histos" means tissue, "pathos" means illness, and "logos" means study is where the word "histopathology" originates [36].

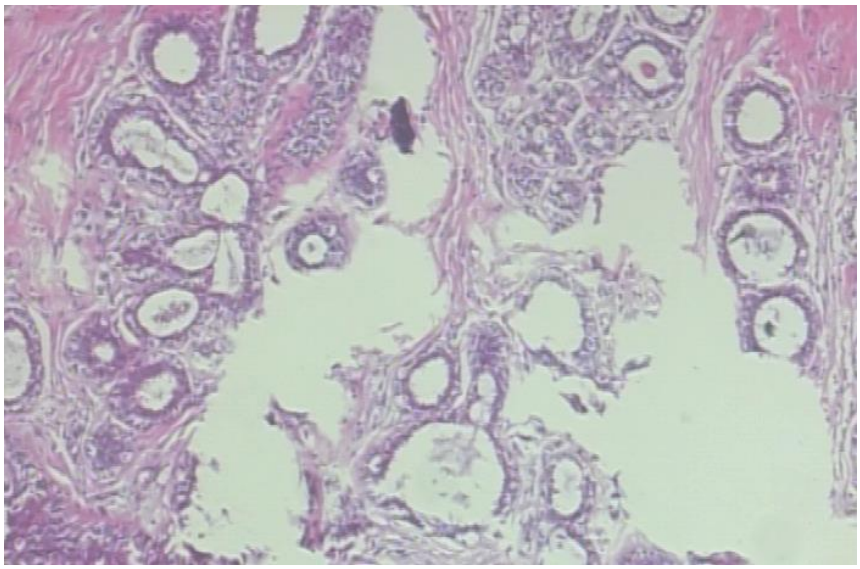

Fig 4.1: Sample from BreaKHis Dataset

Histopathological pictures are microscopic depictions of tissues that are used to diagnose illnesses and anomalies connected to tissues. In particular, tissue samples were taken from suspected lumps or bumps in breast tissue and then observed under a microscope for the BreaKHis dataset. BreaKHis is a collection of therapeutically relevant samples of benign and malignant BCs compiled from microscopic biopsy photos as illustrated in Fig 4.1.

Pathologists can distinguish between distinct forms of BCs, both benign and malignant, by examining the tumor cells under a microscope. As a result, total eight sub classes are found in BreaKHis dataset shown in Fig 4.5. There are presently four histopathologically unique forms of benign breast tumors in the dataset are: adenosis, fibroadenoma, phyllodes tumor, tubular adenoma, and four (BC) malignant tumors are: ductal carcinoma, invasive lobular carcinoma, mucinous carcinoma, and papillary carcinoma samples are shown in Fig 4.2.

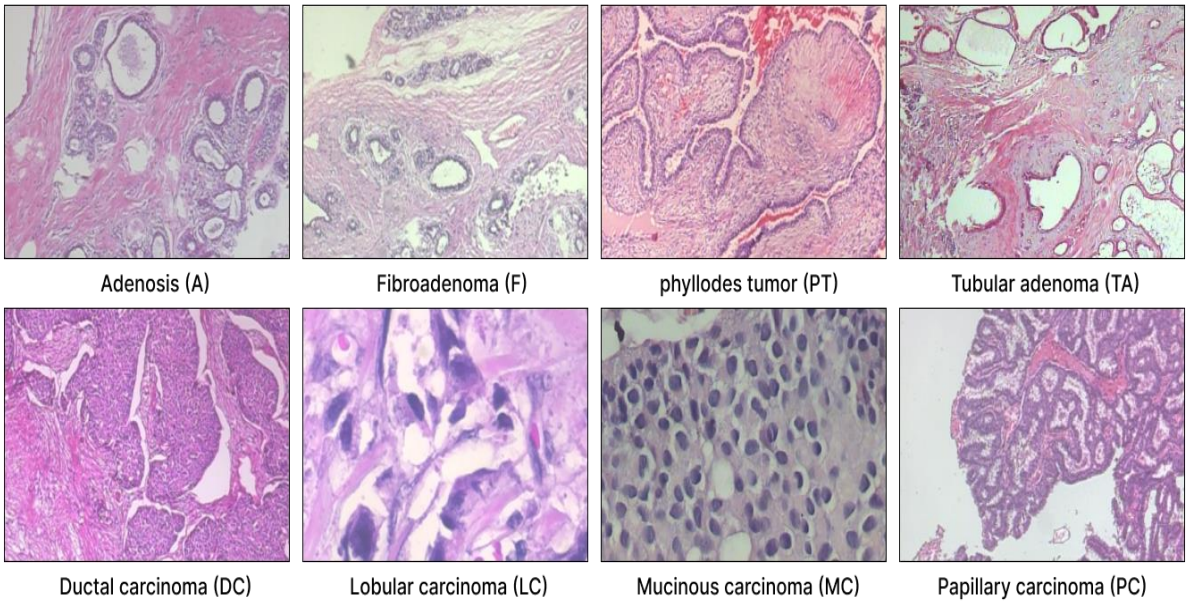

Fig 4.2: Examples of images with labels from the BreaKHis with several magnification levels. Benign instances are shown in the upper row, while malignant ones are shown in the bottom row.

There are 7,909 photos from 82 patients make up the collection, which was created using a variety of magnification factors, including 40×, 100×, 200×, and 400× shown in Fig 4.3. It is noteworthy that 2,480 benign and 5,429 malignant samples are included. More information on the

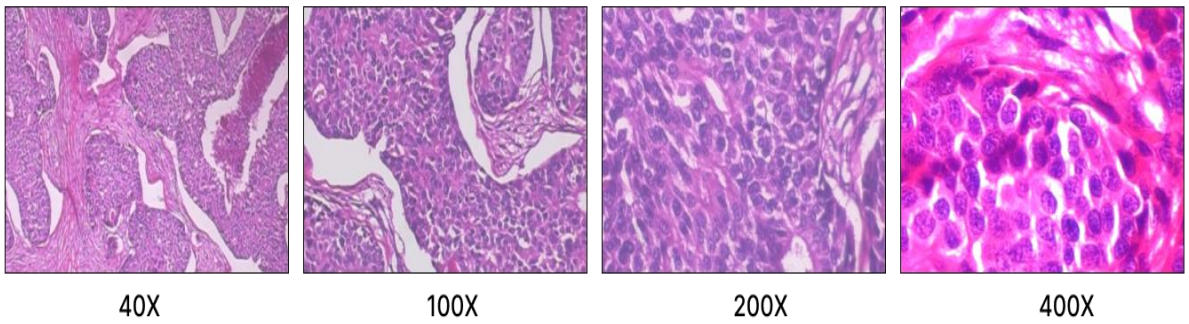

Fig 4.3: Ductal carcinoma from same slide 14-2523 at four different magnifications.

BreaKHis distribution is provided in Table 4.1. Each sample or picture has a size of 700*460 pixels, is stored in PNG format, is 3-channel RGB, and has 8-bit depth in each channel. The sample has picture filenames that provide crucial details about the image, including the magnification factor, patient identifier, tumor class, tumor kind, and biopsy procedure.

Table 4.1: Distribution of BreaKHis dataset

Class	Subclasses	Magnification Levels				Total
		40X	100X	200X	400X	
Benign	A	114	113	111	106	444
	F	253	260	264	237	1014
	PT	149	150	140	130	569
	TA	109	121	108	115	453
Malignant	DC	864	903	896	788	3451
	LC	156	170	163	137	626
	MC	205	222	196	169	792
	PC	145	142	135	138	560
Total		1995	2081	2013	1820	7909

For example, SOB_M_PC-14-1245640 002.png shows the image at 40X magnification, showing a papillary carcinoma type malignant tumor that originated from slide 14-4659 and was

acquired using the SOB process. Samples included in the dataset were obtained via the SOB technique, which is sometimes referred to as excisional biopsy or partial mastectomy[10]. This procedure, which removes a bigger tissue sample, is carried out under general anesthesia at a hospital.

The BreaKHis Dataset's primary folder structure given in Figure 4.4a. Subfolders within each primary categorization folder (malignant or benign) are divided into their respective subclassifications. The malignant folder, for example, comprises samples from ductal carcinoma, lobular carcinoma, mucinous carcinoma, and papillary carcinoma as given in Figure 4.4b. The SOB technique, often referred to as partial mastectomy or excisional biopsy, was used to obtain all samples, which is why the SOB file exists. These samples are further divided into the magnification factors utilized for imaging in each subclassification, which includes folders for every patient. Mucinous carcinoma subclass has 9 patients and each categorized the images into folders according to magnification factor as given in Figure 4.4c.

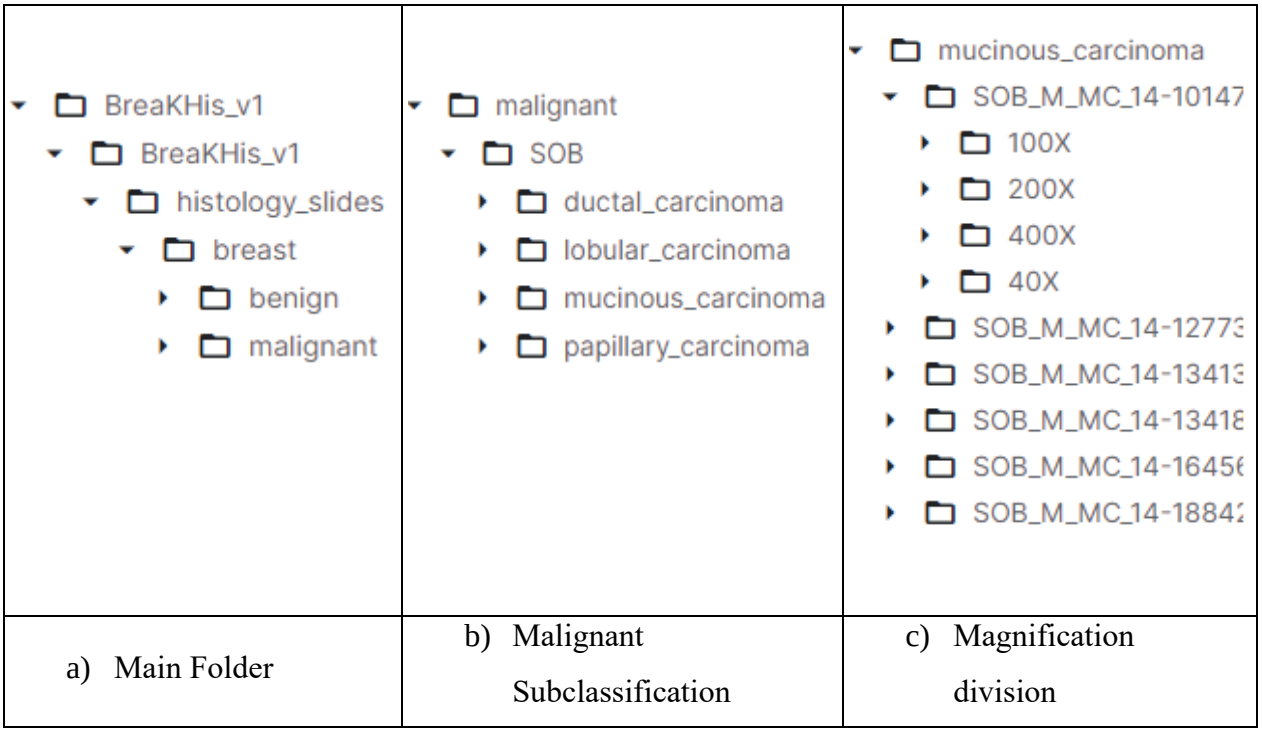

a) Main Folder | b) Malignant Subclassification | c) Magnification division

Fig 4.4: Folder structure of Dataset

[10] It's a surgical procedure in which one or both breasts are removed.

This database was created in collaboration with the P&D Laboratory—Pathological Anatomy and Cytopathology, Parana, Brazil. From January 2014 to December 2014, a clinical investigation was carried out, during which the photos were gathered. Samples in the dataset are prepared for histological analysis and are carefully labeled by P&D Lab pathologists. Hematoxylin and eosin (HE)-stained breast tissue biopsy slides are used to create the samples [91].

The P&D Lab's pathologists gather the samples, prepare them for histological analysis, and label them. The normal paraffin technique, which is often employed in clinical routines, was used in the preparation method. The major objective is to maintain the original molecular makeup and tissue structure so that it can be seen under a light microscope. The entire preparation process consists of phases including clearing, infiltration, trimming, fixation, dehydration, and embedding.

4.2.2 Dataset Limitation:

There are varying quantities of samples in each class due to the imbalance in the dataset. Malignant samples comprise 68.64% of the whole dataset, whereas benign samples make up just 31.36%. Also there's huge imbalance in subclasses. Like in malignant subclasses, the ductal carcinoma has 3451 samples while other types have samples like 626 in lobular carcinoma, 792 in mucinous carcinoma, 560 in papillary carcinoma. This imbalance means that a classifier trained on this data will be biased towards predicting a malignant classification. That said, this complicates the task of implementing a bias-free classifier.

4.2.3 Dataset Advantages:

As histopathology images are obtained directly from regions of interest, feature extraction and segmentation is not needed to done ahead of classification. For this dataset, segmentation is not required; normally, it is done to identify the location of the possible tumor. This greatly simplifies the classifier design as segmentation is not required. The project can go further into the classifier design by allowing for a narrower scope. Additionally, by using histopathological pictures, the entire image's data is utilized for categorization rather than just the segmented portion. This dataset was introduced in 2016 so it can be considered as fairly new dataset. There's no other database with more samples than the BreaKHis. That's why this dataset is considered for this study purpose.

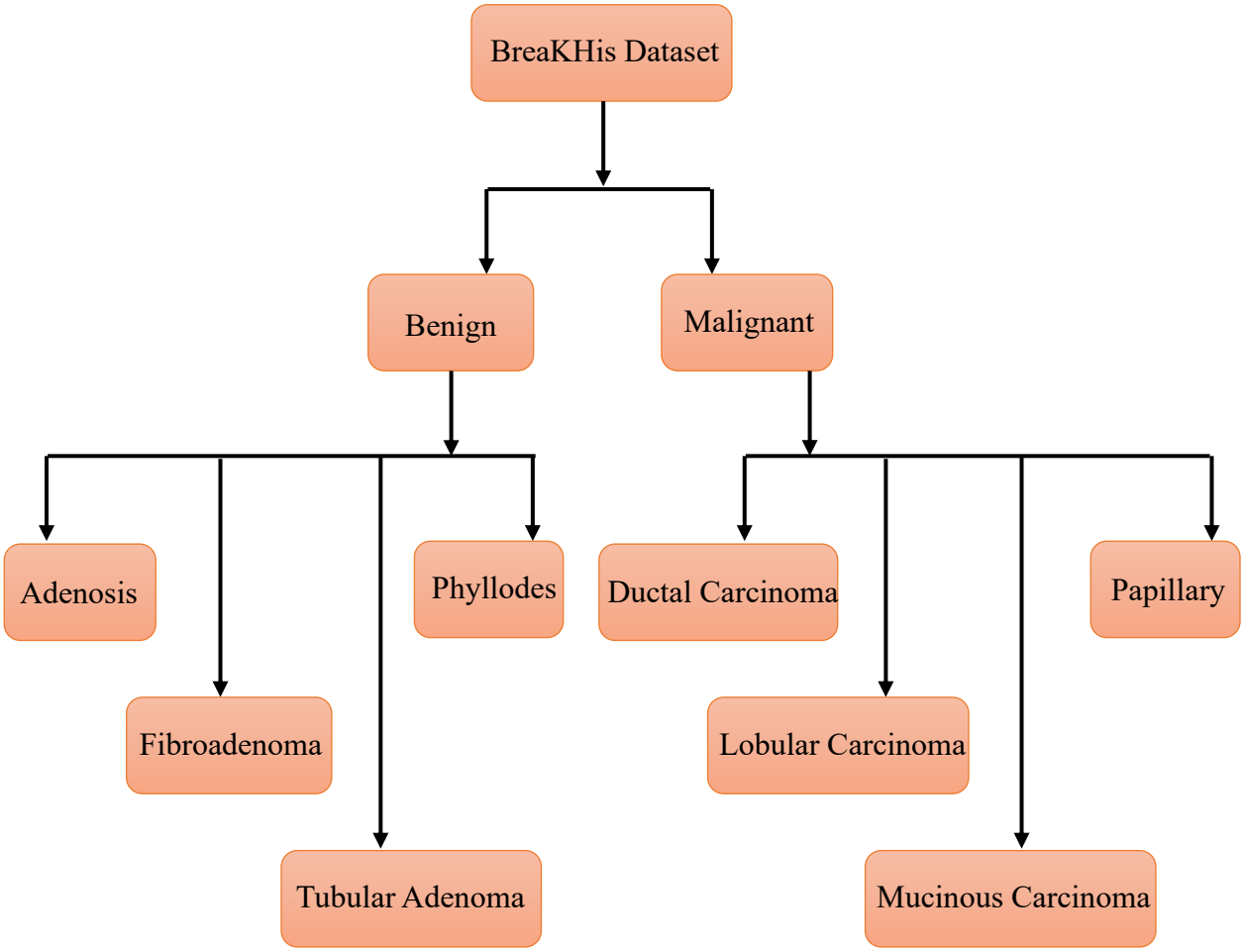

Fig 4.5: Dataset Classes

4.3 Preprocessing:

Preprocessing steps are those steps which are performed to prepare input data before passing data to model. These steps help to remove the none or less informative features, efficient learning and achieve better performance. Different preprocessing steps are performed for classification see figure 4.6.

4.3.1 Down Sampling:

In the very first step a malignant subtype from dataset that is ductal carcinoma is down sampled due to high imbalance between number of samples in classes as mentioned in section

4.2.2. Ductal carcinoma has 46% samples of dataset, which is much greater than other classes samples. This imbalance can makes the model biased which reduces the model accuracy. That's why for avoiding class imbalance down sampling is performed and we take 1146 samples from DC class. After experiments it is noticed that it's the most crucial step in this case.

Fig 4.6: Preprocessing steps workflow

4.3.2 Splitting:

After the first step, Data is divided into training, validation and testing directories with a 80:10:10 ratio independent of their magnifications shown in figure 4.7. Each of these three directories had images from all sub classes. Since the training dataset is what the model is trained on, it is the largest of the three. The test set is used to objectively assess the performance of model as a whole. At the conclusion of every training session, the validation set is utilized for a "unbiased" assessment. The hyperparameters of the model are also adjusted using this evaluation in between epochs. Hyperparameters are variables that influence training yet are unchangeable in the training process.

```
train_images, test_images = train_test_split(images, test_size=0.2, random_state=42)
val_images, test_images = train_test_split(test_images, test_size=0.5, random_state=42)
```

Fig 4.7: Dataset splitting.

As the dataset comprises images from four zoom factors that are 40X, 100X, 200X and 400X. So images are divided with a focus on equal distribution, it means that each split contains data from all the four magnifying factors as shown in figure 4.8. This splitting is done in very earlier step due the reason that moving forward data augmentation is performed. And augmentation must be performed only on training dataset so the testing data remains unseen for model.

```
# Function to copy images and split data by zoom size
def split_data_by_zoom(class_dir, split_dir):
    for zoom in ['100X', '200X', '400X', '40X']:
        for parent_ in os.listdir(class_dir):
            parent_dir = os.path.join(class_dir, parent_)

            zoom_dir = os.path.join(parent_dir, zoom)
            try:
                images = os.listdir(zoom_dir)
            except FileNotFoundError:
                continue  # Skip this zoom level if directory doesn't exist

            # Check if there are enough images to split
            if len(images) < 2:
                continue
```

Fig 4.8: Splitting according to Magnification levels

4.3.3 Resizing:

After splitting the next step in preprocessing is that images resizing. The dataset's 700*460 mega pixel raw images were all resized to 224*224 mega pixels in order to fit the YOLOv5x-cls input layer. And then data augmentation is applied.

4.3.4 Augmentation:

Augmentation offers the increasing of dataset size synthetically for few reasons. The first is that for achieving a good performance, as CNN models require a lot of data for training so data is increased with various techniques and the other is to avoid overfitting[11] and imbalance. Augmentation increases dataset by creating copies(over sampling) of existing dataset. Various techniques (such as affine transformations, kernel filters, color transformation, GANs etc.) are used for augmentation which make changes in original image. Each technique produces different changes. We can create millions of copies of dataset using augmentation. In this work, we have applied augmentation on training dataset only, so the testing dataset remains unseen. And we have used total of three augmentation techniques, two of which are affine transformations vertical flipping and horizontal flipping and a color transformation that is color invert shown in figure 4.9.

[11] It's a situation in which model performs well on the training data but couldn't predict well on unseen data.

For binary classification, augmentation is applied separately on benign and malignant data. The total number of images in benign class were 2368 and after 80% split there are 1894 training images

```
iaa.Fliplr(0.5), # flip image horizontally
iaa.Flipud(0.5), # flip image vertically
iaa.Invert(0.05, per_channel=True), # invert color channels
```

Fig 4.9: Augmentation techniques

on which augmentation is applied and its size is increased to 4585 images. In malignant class there were 2424 training images and after augmentation it increased to 7008 images.

4.3.5 Balancing:

After augmentation, class balancing is performed to make each subclass equal in number of counts by randomly up-sampling images according to max count of images in any class. For example for benign tumor there were 1071 samples for phyllodes, 1050, 1578, 886 for adenosis, fibroadenoma, and tabular respectively after augmentation. In these max or highest count is 1578 so all other types are up-sampled and each benign subclass then have 1578 samples.

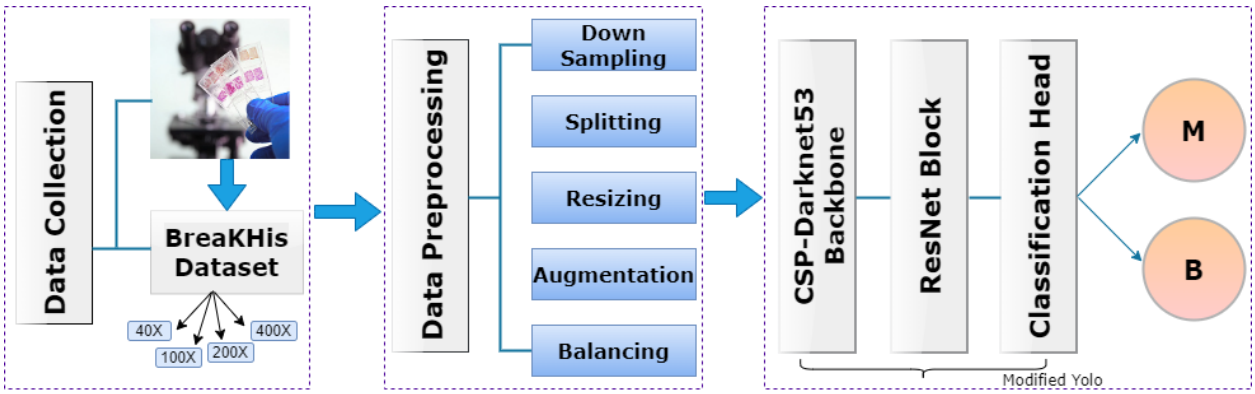

Fig 4.10: Workflow of proposed methodology

4.4 Proposed Model:

The present research study primarily focuses on classification of BC from Histopathological images using YOLO model, along with incorporating a modification for extracting more complex features. ResNet block has been integrated after the backbone of

architecture of YOLO model and before to enhance capabilities to learn more complex features and faster convergence.

4.4.1 YOLO:

The model was implemented using PyTorch which is a famous framework of DL developed by Facebook. The first YOLO model a object detection technique was developed in 2016 by Ultralytics, and afterwards are the variations of 1st model. In 2020 YOLOv5 model was developed which also supports classification tasks from August 2022. The class probabilities and bounding box collection are predicted by the YOLO neural network architecture. The complete image is first divided into several grids of various sizes, and then anchor boxes are created using predetermined scale and size in each grid of the input image. Rather of creating boundary boxes, the model predicts class probabilities for classification. Yolov5-cls is pretrained on ImageNet dataset, for each input it provides a probability for all class labels.

YOLOv5 detection architecture has 3 parts: Backbone which used CSP-Darknet53 structure which refers to CNN architecture so is used to extract hierarchical features from histopathological images and represent the features at different levels. Darknet is a CNN architecture specially designed for YOLO. CSP-Darknet53 involves 53 convolutional layers of 3*3 kernel, batch normalization and sigmoid Leaky Relu function, C3 structure. Batch normalization prevents the network overfitting and also accelerate or speed up model convergence. Gradient changes are integrated into feature map through C3 structure which reduces computation and maintain accuracy. A SPPF block is added over CSPDarkNet53 because it increases receptive field and separates the most important or significant features and it also don't affect model's speed. The Neck part of YOLO is used for aggregation of parameters or refining features from different scales of backbone CSP-PAN and the detection Head makes bounding boxes and gives probability for each class.

But for classification YOLOv5 does not have all these three modules, classification model only involves a CSP-Darknet53 based backbone having convolutional layers and bottleneck for extracting the hierarchical features and then a classification head which categorizes the full image into one of the defined classes. Its like backbone --> classification head. Darknet53 is a variation

of CNN models which is designed specifically for YOLO model to enhance its capability of extracting hierarchical features.

As Darknet is based on CNN models so it uses the basics of CNN for extracting features. Each convolutional layer in YOLO involves three operation which are convolution operation, Batch Normalization (BN) and SiLU activation function. Convolutional operations where filters are passed over the images to extract useful information from the image. Filters play a very important role in feature learning. Network automatically adjust filters and optimize them through back propagation. These filters move over the input pixel with a stride value and filter is convolved with input pixels and results are aggregated, this operation is called convolution operation and it generates features maps. After the convolution operation there is BN which is used to avoid over-fitting. SiLU is activation function that utilizes sigmoid function multiplying with itself. Darknet based backbone consists of multiple convolution layers which keep on extracting features from input data, starting layers extract basic features like edge details, moving forward as the model becomes deep it extracts more complex and appropriate features from input data. After performing convolutional operations all the feature maps are flatten to create a single 1D array which is passed to fully connected layers for classification. Flatten array is used an input to fully connected layers.

Fully connected layers are a dense neural network which contains dense network of neurons. These are called fully-connected because every neuron in a single fully connected layer is connected to all the neurons in previous layer and all the neurons in next layer. These fully-connected layers are responsible for learning weights to associate features to particular class or label. Classification head includes convolution layer, Dropout layer, linear and adaptive average pooling2D function, this adaptive pooling is used to make the model such a way that can adjust pooling window size according to the dimensions of input image. It helps to maintain the spatial information before feeding data to final or last fully connected layer which classifies features.

YOLOv5 model has different variation like YOLOv5n, YOLOv5s, YOLOv5m, YOLOv5l, YOLOv5x. All variations differ due to their sizes, parameters involved, number of features they can extract and speed. So, in this study we have implemented YOLOv5x-cls that is the extra large variation of YOLOv5. Although the larger model involves more parameters and is deeper but it also provide good performance and accuracy.

4.4.2 Modified YOLO Architecture:

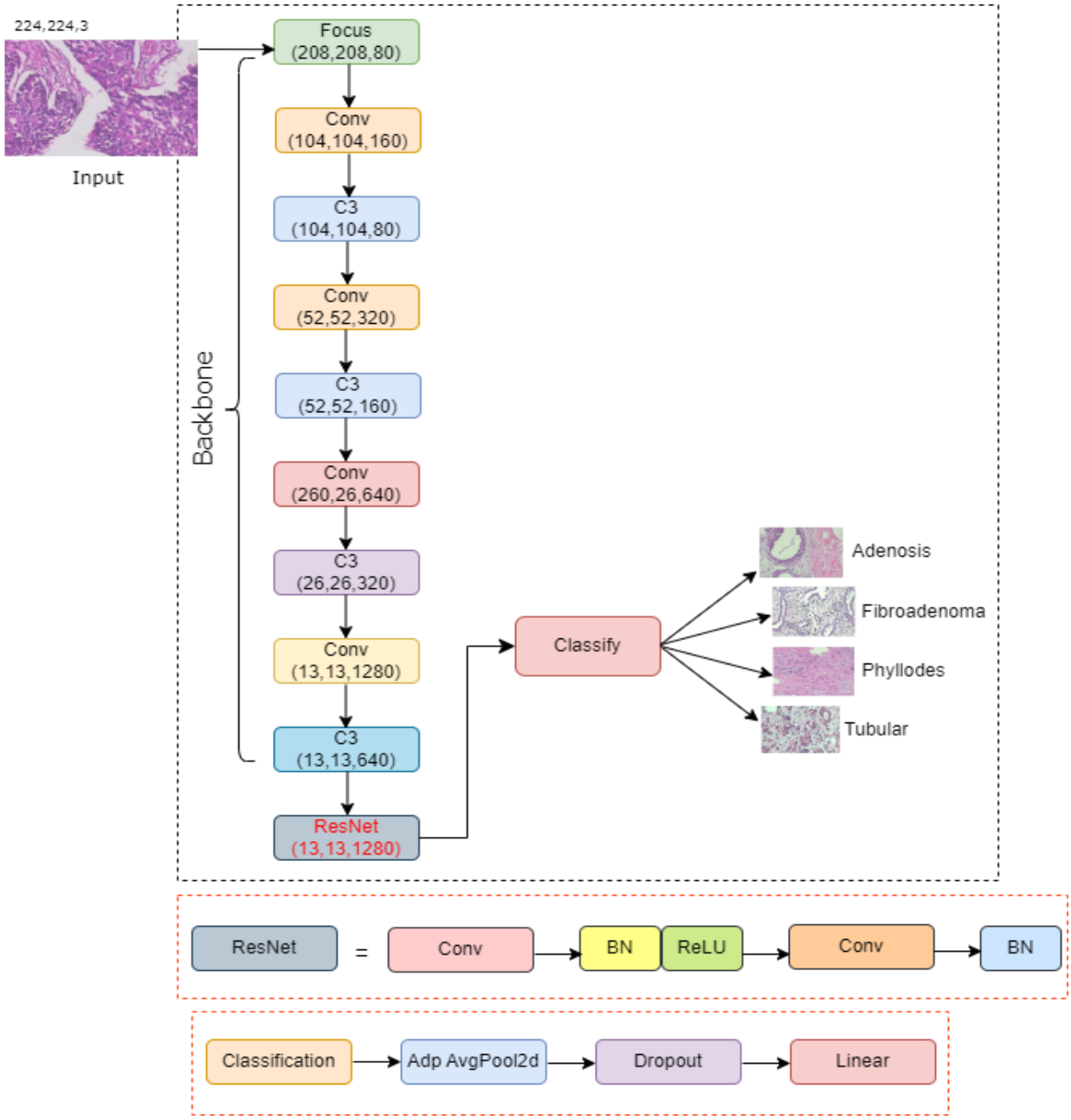

Fig 4.11: Modified architecture of YOLOv5

This work proposed a YOLOv5 model with ResNet feature extractor for classifying BC into benign and malignant classes as well as further classify to their subclasses. In architecture ResNet block is incorporated in sequence into the existing architecture in sequence after the CSPDarknet53 backbone and before classification head to extract more features from complex

histopathological images. Its like backbone --> ResNet block --> classification head. The modified architecture of YOLOv5x is presented in Figure 4.11.

The Resnet block enhances model's feature learning capabilities. Residual connections help to learn and propagate features effectively. Adding more layers aid the model to learn more complex representations. It involves convolution layers and batch normalization which helps extracting more complex features. The block involves convolutional layers with kernel size 3*3, batch normalization and ReLU activation function which helps model bring non-linearity. ReLU activation function changes all to negative values to 0 and remains other values unchanged. ResNet blocks aid in collecting and maintaining high-level features because of their skip connections and residual learning capabilities. Residual connections provides smoother gradient flow and this helped to faster convergence while training. The YOLOv5 backbone facilitates an initial feature extraction and ResNet block boosted the model's ability to learn more complicated and abstract features and this particularly helped in classifying BC subclasses. The backbone consists of bottleneck blocks which processes the image and detect features. The added block improved the model's accuracy, results discussed in chapter 5 to diagnose more precisely.

4.5 Training process:

For training we build 3 models one for binary classification, one for malignant subclass classification and other for benign subclass classification. Before model training few preprocessing steps were introduced to improve model's performance like down sampling was introduced only for model designed for malignant subclass classification because malignant class has a huge imbalance between subclasses. Then dataset is splitted into training and testing sets, 80% for training, 10% for validation and 10% for testing. In third step resizing is performed, original images were of size 700*460 which are reduced to a size of 224*224 because it's the required size for YOLOv5x-cls. Augmentation was used to synthetically increase dataset size because CNN based models require large data for learning and performing better and then classes are balanced as last preprocessing step to balance all classes according to max image count. After completing all these preprocessing steps the dataset is given to model for training, input shape given to model is 224*224*3.

For classification each image is given label according to the folder in which it is saved. Giving labels from folder name involves benefits like class labels can be clearly defined through folder structure and there are less chances of mistake that manual labelling can have. We have tried and tested different experiments to find which techniques goes well with out model. We have performed experiments without augmentation and down sampling but didn't achieved much good results for those cases. Also we have trained with different image sizes but didn't find much difference in results. For optimal results, parameters used are discussed like, For malignant classes we had total 7008 training images, for benign classes we had 6312 training examples and for binary class we had 8684 training samples. Epochs for training were set to 300, 0.001 learning rate and a batch size of 64. The classification or fully connected layers uses total 1024 filters, with stride = 1, filter size = 1, and uses SiLU activation function to classify images into required classes. The output layer of model consists of 4 channels for subclass classification models and 2 channels for binary classification.

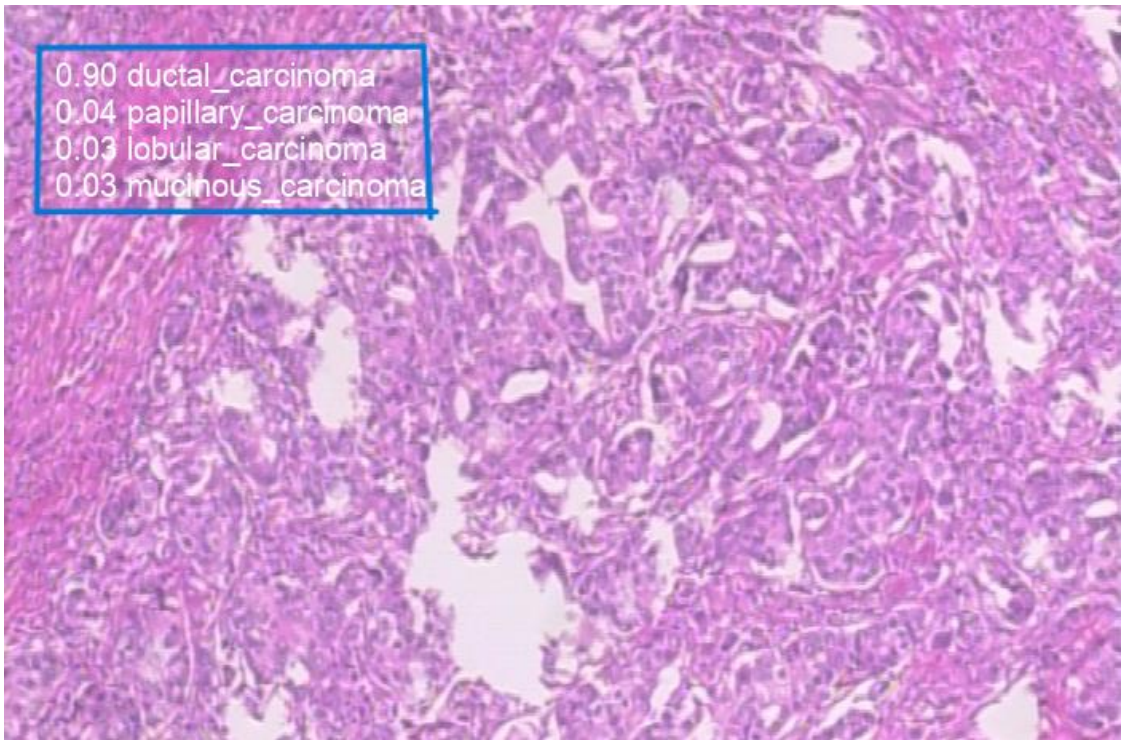

Fig 4.12: Result image with class probabilities

For Evaluation, performance accuracy and train test losses were tracked using wandb as well as using Tensorboard logs. After completing the training the inference on test images is

conducted using the best saved weights during the training. And the final output are the images showing probability for all classes involved shown in figure 4.12.

4.6 Summary:

This chapter discussed about the proposed methodology with initial steps and proposed model with architecture. Like section 4.2 discusses in detail about dataset, how its collected, its pros and cons, and why this dataset has been selected for this study. Moving forward section 4.3 discusses the preprocessing steps performed on dataset to increase model efficiency. Section 4.4 discussing proposed YOLO model and then in section 4.6 all the training details are given that which parameters were selected for training or fine tuning the modified YOLO for BC classification.

CHAPTER 5

Results and Discussion

5.1 Experimental Setup:

For implementing classifier for BC classification preprocessing relevant tasks are performed on Google Collab and PyTorch framework was used on a GPU machine having NVIDIA Quadro RTX 4000 GPU with 8GB of RAM for training experimentation. For training

Table 5.1: Experimental setup

PARAMETER	VALUE
Image size	224
Epoch	300
Batch size	64
Model	YOLOv5x-cls.pt

parameters were set to 224*224 image seize, 300 epochs and 64 batch size.

5.2 Evaluation Metrics:

In this study we used accuracy, train/test loss graphs and confusion matrix for the evaluation of our proposed model which is bench mark criteria. To measure overall performance of model accuracy metric is used.

$$\text{Accuracy} = \frac{\text{Number of correct predictions}}{\text{Total number of predictions}}$$

But only accuracy metrics is not enough for evaluating the robustness of a model. So confusion matrix is calculated also. The number of successfully categorized targets is represented by the content of the matrix at diagonal position i = j. Therefore, it seems sense that the Confusion Matrix's non-diagonal places would want to be as minimal as feasible. An illustration of a confusion matrix is presented in Figure 5.1.

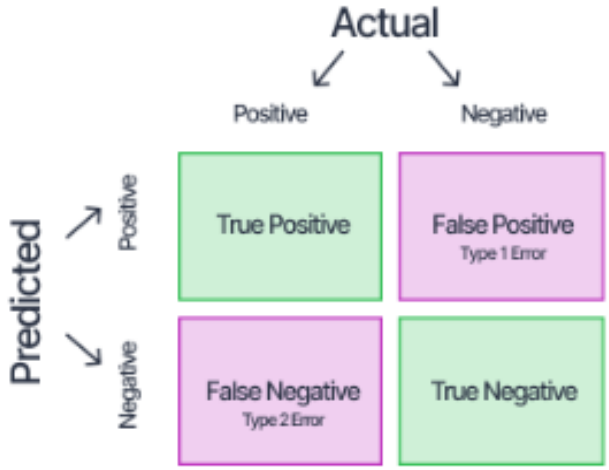

Fig 5.1: Confusion Matrix

5.3 Experimental Results:

This section shows the results achieved using our implemented model. For tracking the performance of models training process, we evaluated accuracy, classification report as well as confusion matrix. Binary Classification model: Firstly model is trained for binary classification of BC into benign or malignant. Figure 5.2 shows the testing accuracy of model. For classifying BC test images confusion matrix is presented in figure 5.3, 11 images were misclassified indicating that achieved an accuracy of 99%.

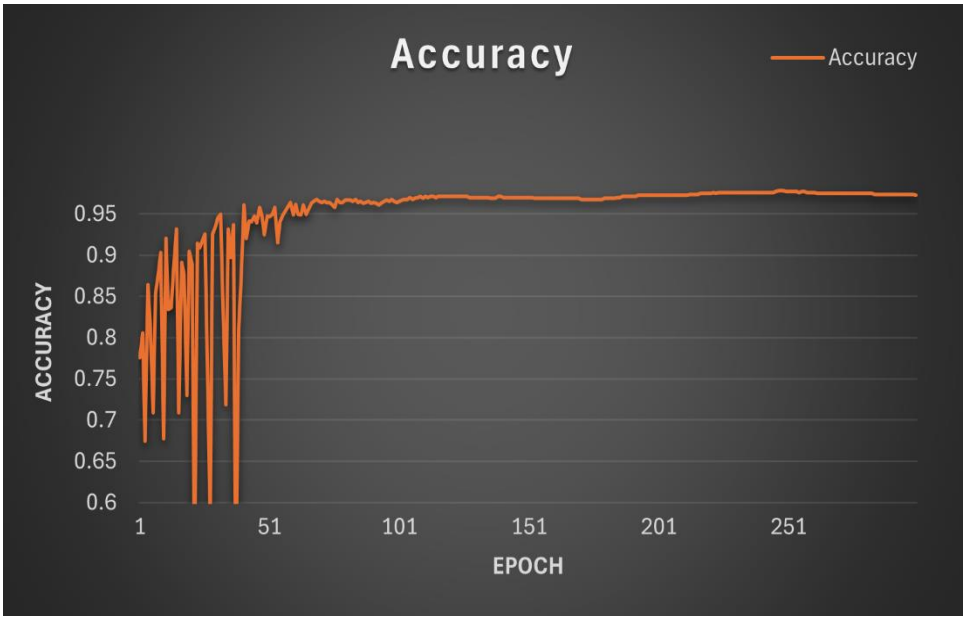

Fig 5.2: Binary class accuracy graph

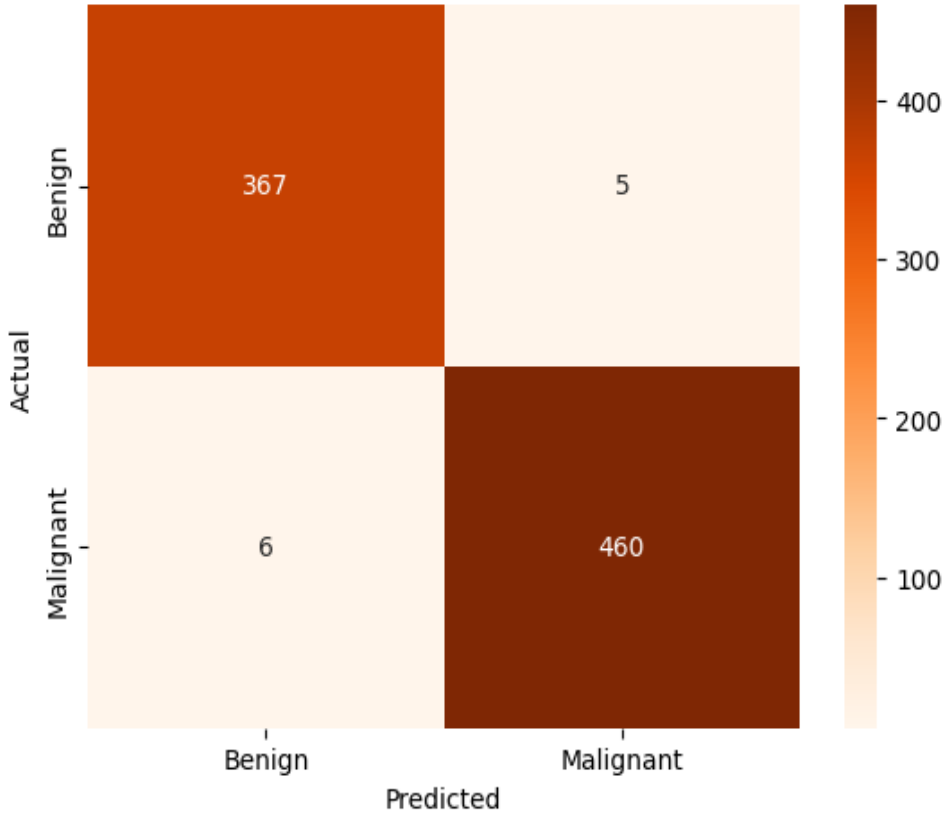

Fig 5.3: Binary class Confusion matrix

Malignant multiclass Classification model: Second model is trained for classifying subclasses of malignant tumor. There are four subclasses of malignant tumor given in dataset, figure 5.4 shows test accuracy graph and confusion matrix is presented in figure 5.5 for this case. Six images are misclassified while achieving a test accuracy of 98% .

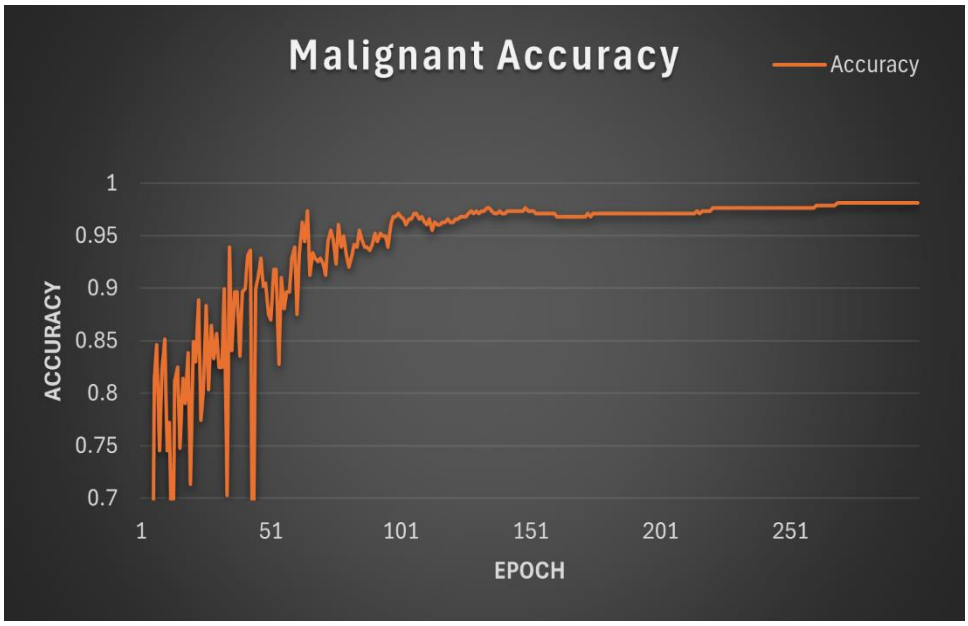

Fig 5.4: Malignant class accuracy graph

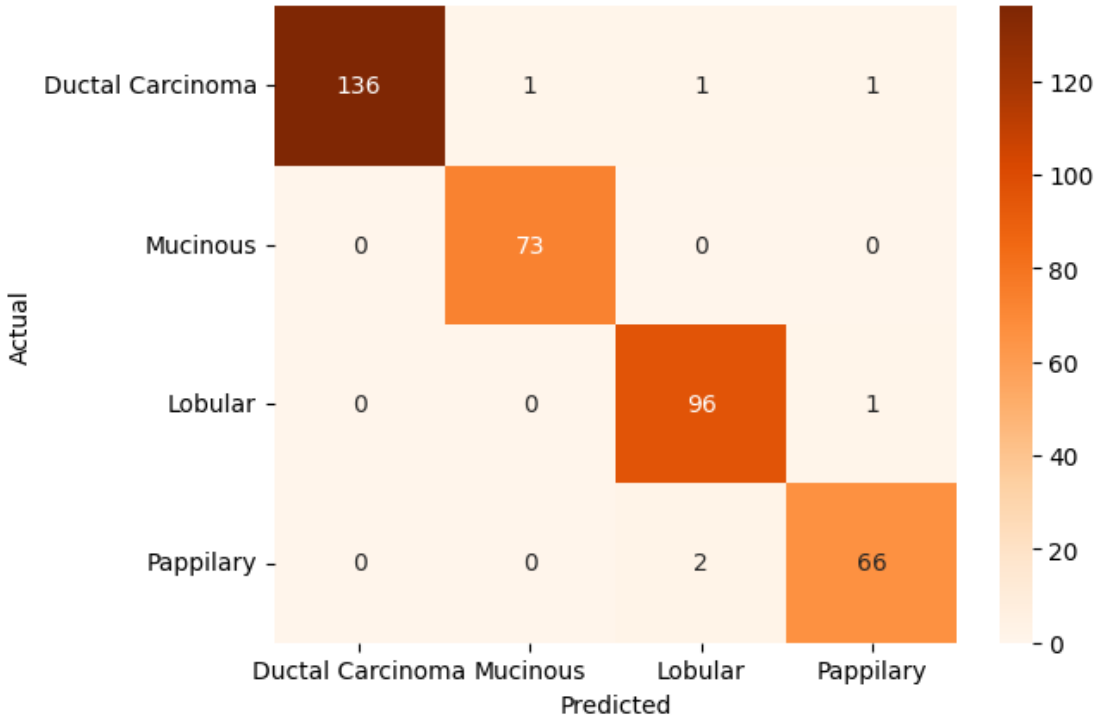

Fig 5.5: Malignant class Confusion matrix

Benign multiclass Classification model: Third model is trained for classifying subclasses of benign tumor. For benign case 8 images were misclassified shown in figure 5.7 with a test accuracy of 97% which is presented in figure 5.6.

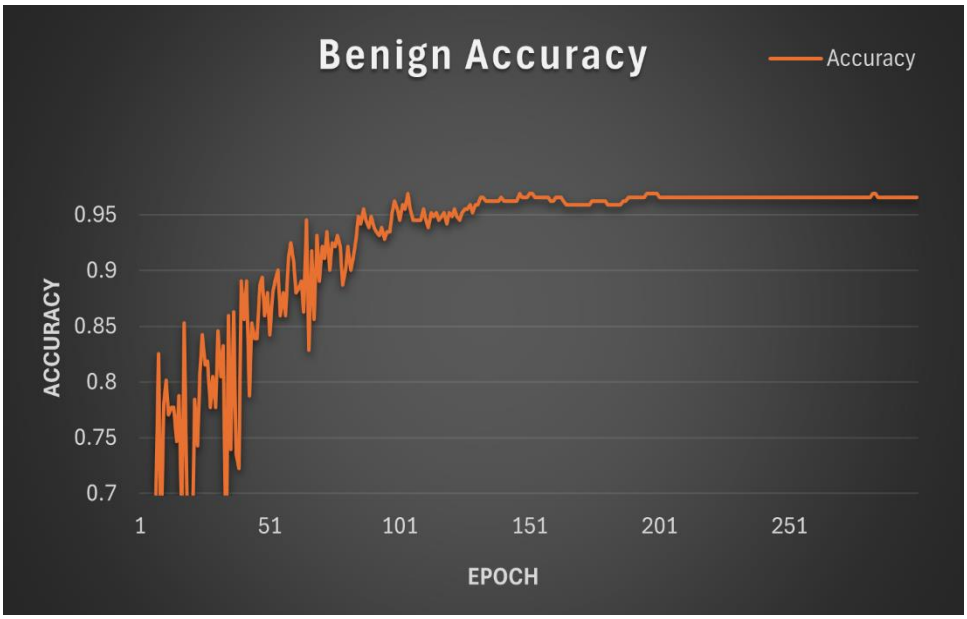

Fig 5.6: Benign class accuracy graph

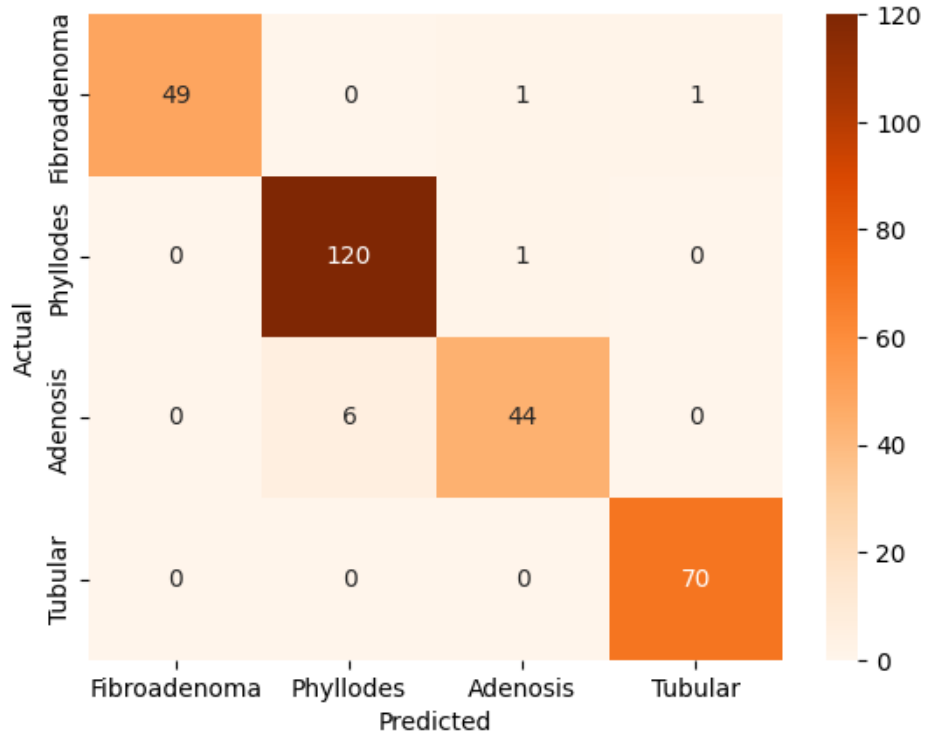

Fig 5.7: Benign class Confusion matrix

5.4 Discussion:

To determine the best influenced train test split three different splitting arrangements 90%:10%, 80%:20%, 70%:30% are used because it has a larger impact on the performance of CNN based models. Best results achieved using a 80% training set and 10% testing set, the classifier from this research study achieved an accuracy of 99% for binary classes, 97% for benign subclasses and 98% for malignant subclasses classification. Moreover, it is observed that imbalance data also affects the model's performance badly, if there's more samples in one class than the other the model can be biased towards that class with more samples. Like in BreaKHis dataset used in this study there's a huge imbalance between classes. It has 2368 images in benign class and 5429 images in malignant class so when we tried to use this data as it is proposed model performed very badly. So overcome this imbalance between classes it's necessary to do some technique which can balance the classes so we opted down sampling technique and down sampled malignant class to 3101 images.

Zewdie et al. [10] developed a binary and multi class classifier model and their model achieved an accuracy of 96.75%, 96.7% and 95.78% for binary, benign and malignant classes respectively using the same dataset used in this study. Unlike our model and the model developed by Zewdie et al. model, the model's performances in a paper by Tummala et al. [88] are separated by magnification scales. A two-class as well as eight class classifier model was developed and their two-class model achieved an accuracy of 99.6%, for eight classes their model achieved best accuracy at 40X which was 95.5%. But its difficult to exactly compare their accuracy with ours due to their separated results. The average accuracy achieved by their model was 96% although this accuracy is good, but still its lower than our model. Jannesari et al. [74] also implemented a multi class model in which their two class model achieved an accuracy of 98.7% while benign class achieved 94.8% and malignant class achieved 96.4% accuracy.

Li. et al. developed a 2 phase embedded fusion mutual learning model. Where in the end-to-end phase at first stage 2 heterogenous networks were used for the mutual learning of features. And then ensemble the classifier which completes the training procedure, at 2nd stage they extracted intermediate features of two networks. And used adaptive feature fusion technique for fusion of two networks features. At 3rd stage they transfer the fused features back to network for strengthening their training procedure, and then at 4 they calculated class probabilities of fusion classifier to obtain classification results. In non-end-to-end phase they used the deep-level extracted features for training traditional classifiers to classify images into two classes. Although their model achieved a good accuracy but model is very complex as well as also dependent on magnification levels, which means that model could not perform well on other magnification levels.

The proposed work is also compared with ResNet50, InceptionV3 and InceptionResNetV2. For these models we have used the same preprocessing pipeline. ResNet achieved 93% accuracy for binary class, 86% and 82% accuracy for benign and malignant respectively. 91.8%, 81% and 83% of accuracy for binary, benign subclasses and malignant subclasses respectively is achieved by InceptionV3. InceptionResNetV2 provides an accuracy of 96%, 87%, 81% for binary, benign subclasses and malignant subclasses respectively. Comparison shows that modified YOLOv5 model is more accurate and perfect choice for classification of BC. From Table 5.2 it can also be observed that our model achieves better accuracy for benign and malignant classes.

Table 5.2: Breast cancer classification results comparison

Model	Binary class	Malignant class	Benign class
ResNet50	96.75%	96.70%	95.78%
Swin Transformer	99.60%	96%	96%
BMIC_Net	95.48%	92.45%	95%
Inception	91.80%	83%	81%
InceptionResNetV2	96%	81%	87%
Ours	**99.00%**	**98%**	**97%**

CHAPTER 6

Conclusion

Breast Cancer is the deadliest cancer and its cases are increasing every year. So in this study, a binary and multiclass classification model was developed for early diagnosis of BC which classifies a set of Histopathological breast-images into Benign and Malignant classes and their subclasses. Compared to binary classification, multi-classification has more clinical value since it offers additional information about patients' health issues, which reduces pathologists' workloads and helps pathologists create more effective treatment plans. The YOLO model with ResNet feature extractor has been used for the classification. The YOLOv5 model's backbone extract hierarchical features from input images, a ResNet block is incorporated in the architectural pipeline of YOLOv5 to extract more features from complex images. Those features are then used by classification head to classify more precisely.

This work has developed three models that make use of the hierarchical characteristic of the YOLO model and the advantages of local and global domain information. First model for classifying images to benign or malignant class. Second model classifies the malignant sub-classes, for this model there's an additional preprocessing step was performed that is down sampling. Due to high imbalance in malignant classes in dataset, down sampling need to perform. And the third

model classifies the benign classes. For experiments this study has utilized BreaKHis dataset. Most of existing studies for multiclass performed magnification dependent classification that makes the model dependent that it cannot classify images with different zoom level. Proposed model performs the magnification independent classification which makes the model more generalized that it can diagnose and classify BC from any magnification powered digital histopathology image.

The outcomes demonstrated that our suggested technique may reliably outperform previous research in terms of performance. In addition to the accuracy data, we also recorder the precision, recall, and F1-Score values in this study. According to the experiments, the modified YOLOv5 performs the best on given dataset. Binary classification model provides accuracy of 99%, and 0.99 Precision, F1-Score, and Recall value. For Malignant subclass classification model achieved best accuracy of 98%, average 1.00 precision and recall 0.99 f1-score. For Benign subclasses model gained 99% accuracy, average 1.00 precision and recall, 0.99 f1-score.

Lessons learned from this work includes that data unbalancing effects a lot on model's performance badly, when dataset is small Data augmentation can play a great role for improving the model's accuracy. Rather than choosing a complex model that increases the computational cost of model and takes a lot of training time, such model is not preferred in medical diagnosis, a simpler model can reduce computational cost while achieving a good accuracy for classification on BreaKHis dataset.

Getting a correct diagnosis as soon as possible is crucial to increasing the probability of breast cancer patients surviving. The death rate from breast cancer may be lowered with the use of this classifier. It is hoped that this automatic classifier will assist save lives and that this work will serve as a guide for future researchers with similar objectives.

6.1 Future Work:

In future, we can build and deploy a website application that can be used for clinical assessment and helps pathologists in their findings. Moreover, for increasing models' performance accuracy we can use GANs for generating synthetic data instead of augmentation.

References:

[1] "Understanding what cancer is: Ancient Times to present. American Cancer Society. https://www.cancer.org/cancer/understanding-cancer/history-of-cancer/what-is-cancer.html."

[2] R. Lakhtakia, "A brief history of breast cancer: Part I: Surgical domination reinvented," *Sultan Qaboos Univ Med J*, vol. 14, no. 2, p. e166, 2014.

[3] "Breast cancer. WCRF International. https://www.wcrf.org/diet-activity-and-cancer/cancer-types/breast-cancer/."

[4] "Breast cancer facts and statistics 2023. https://www.breastcancer.org/facts-statistics."

[5] C. C. medical professional, "Benign tumor: Definition, types, Causes & Management, from https://my.clevelandclinic.org/health/diseases/22121-benign-tumor."

[6] Bukun, "Breakhis. https://www.kaggle.com/datasets/ambarish/breakhis."

[7] "Importance of breast cancer awareness in Pakistan. https://shifainternationalpatients.com/importance-of-breast-cancer-awareness-in-pakistan/."

[8] "PR 223 - international agency for research on cancer. https://www.iarc.who.int/wp-content/uploads/2018/07/pr223_E.pdf."

[9] J. Welsh, "History of breast cancer: Background and notable breakthroughs. from https://www.verywellhealth.com/history-of-breast-cancer-5207255 ."

[10] E. T. Zewdie, A. W. Tessema, and G. L. Simegn, "Classification of breast cancer types, sub-types and grade from histopathological images using deep learning technique," *Health Technol (Berl)*, vol. 11, no. 6, pp. 1277–1290, Nov. 2021, doi: 10.1007/s12553-021-00592-0.

[11] W. N. Street, W. H. Wolberg, and O. L. Mangasarian, "<title>Nuclear feature extraction for breast tumor diagnosis</title>," R. S. Acharya and D. B. Goldgof, Eds., Jul. 1993, pp. 861–870. doi: 10.1117/12.148698.

[12] P. Pramanik, S. Mukhopadhyay, S. Mirjalili, and R. Sarkar, "Deep feature selection using local search embedded social ski-driver optimization algorithm for breast cancer detection in mammograms," *Neural Comput Appl*, vol. 35, no. 7, pp. 5479–5499, 2023.

[13] O. Ginsburg *et al.*, "Breast cancer early detection: A phased approach to implementation," *Cancer*, vol. 126, no. S10, pp. 2379–2393, May 2020, doi: 10.1002/cncr.32887.

[14] K. E. Lukong, "Understanding breast cancer – The long and winding road," *BBA Clin*, vol. 7, pp. 64–77, Jun. 2017, doi: 10.1016/j.bbacli.2017.01.001.

[15] "History of cancer epidemiology: 18th century to present. American Cancer Society. https://www.cancer.org/cancer/understanding-cancer/history-of-cancer/cancer-epidemiology.html."

[16] S. Brechon, "A brief history of breast cancer. Maurer Foundation. https://www.maurerfoundation.org/a-brief-history-of-breast-cancer/."

[17] “Milestones in cancer research and Discovery. National Cancer Institute. https://www.cancer.gov/research/progress/250-years-milestones.”

[18] R. Singal, R. P. Singal, A. Mittal, S. Sangwan, and N. Gupta, “Sir Astley Paston Cooper,” *Indian Journal of Surgery*, vol. 73, no. 1, pp. 82–84, Jan. 2011, doi: 10.1007/s12262-010-0177-2.

[19] F. C. Koerner, “A brief historical perspective on the pathology of the breast: from cheatle to azzopardi and beyond,” *Semin Diagn Pathol*, vol. 21, no. 1, pp. 3–9, Feb. 2004, doi: 10.1053/j.semdp.2003.10.008.

[20] “Antonie van Leeuwenhoek. Encyclopædia Britannica, inc. https://www.britannica.com/biography/Antonie-van-Leeuwenhoek.”

[21] R. H. Young and D. N. Louis, “The Warrens and other pioneering clinician pathologists of the Massachusetts General Hospital during its early years: an appreciation on the 200th anniversary of the hospital founding,” *Modern Pathology*, vol. 24, no. 10, pp. 1285–1294, Oct. 2011, doi: 10.1038/modpathol.2011.132.

[22] R. Lakhtakia and R. F. Chinoy, “A brief history of breast cancer: Part II-Evolution of surgical pathology,” *Sultan Qaboos Univ Med J*, vol. 14, no. 3, p. e319, 2014.

[23] “Timeline: The evolution of breast cancer: 3000 BCE to 2016. https://www.researchgate.net/figure/Timeline-The-evolution-of-breast-cancer-3000-BCE-to-2016_fig1_313020660.”

[24] R. L. Egan, “Mammography, An Aid to Diagnosis of Breast Carcinoma,” *JAMA*, vol. 182, no. 8, Nov. 1962, doi: 10.1001/jama.1962.03050470017004.

[25] H. Holmström, “The Free Abdominoplasty Flap and Its Use in Breast Reconstruction: An Experimental Study and Clinical Case Report,” *Scand J Plast Reconstr Surg*, vol. 13, no. 3, pp. 423–427, Jan. 1979, doi: 10.3109/02844317909013092.

[26] Radiological Society of North America (RSNA) and American College of Radiology (ACR), “Breast cancer. Radiologyinfo.org. https://www.radiologyinfo.org/en/info/breast-cancer.”

[27] Radiological Society of North America (RSNA) and American College of Radiology (ACR), “Breast cancer. https://www.radiologyinfo.org/en/info/breast-cancer.”

[28] R. F. Brem, M. J. Lenihan, J. Lieberman, and J. Torrente, “Screening breast ultrasound: past, present, and future,” *American Journal of Roentgenology*, vol. 204, no. 2, pp. 234–240, 2015.

[29] “Breast Ultrasound. Johns Hopkins Medicine. https://www.hopkinsmedicine.org/health/treatment-tests-and-therapies/breast-ultrasound.”

[30] R. M. Mann, N. Cho, and L. Moy, “Breast MRI: state of the art,” *Radiology*, vol. 292, no. 3, pp. 520–536, 2019.

[31] “Breast cancer. Mayo Clinic. https://www.mayoclinic.org/diseases-conditions/breast-cancer/diagnosis-treatment/drc-20352475.”

[32] “Breast biopsy. Mayo Clinic. https://www.mayoclinic.org/tests-procedures/breast-biopsy/about/pac-20384812.”

[33] E. A. M. O’Flynn, A. R. M. Wilson, and M. J. Michell, “Image-guided breast biopsy: state-of-the-art,” *Clin Radiol*, vol. 65, no. 4, pp. 259–270, Apr. 2010, doi: 10.1016/j.crad.2010.01.008.

[34] S. Mitra and P. Dey, “Fine-needle aspiration and core biopsy in the diagnosis of breast lesions: A comparison and review of the literature,” *Cytojournal*, vol. 13, p. 18, Aug. 2016, doi: 10.4103/1742-6413.189637.

[35] H.-P. Chan, R. K. Samala, and L. M. Hadjiiski, “CAD and AI for breast cancer—recent development and challenges,” *Br J Radiol*, vol. 93, no. 1108, p. 20190580, Apr. 2020, doi: 10.1259/bjr.20190580.

[36] C. Kaushal, S. Bhat, D. Koundal, and A. Singla, “Recent Trends in Computer Assisted Diagnosis (CAD) System for Breast Cancer Diagnosis Using Histopathological Images,” *IRBM*, vol. 40, no. 4, pp. 211–227, Aug. 2019, doi: 10.1016/j.irbm.2019.06.001.

[37] R. Rashmi, K. Prasad, and C. B. K. Udupa, “Breast histopathological image analysis using image processing techniques for diagnostic purposes: A methodological review,” *J Med Syst*, vol. 46, no. 1, p. 7, Jan. 2022, doi: 10.1007/s10916-021-01786-9.

[38] N. O’Mahony *et al.*, “Deep Learning vs. Traditional Computer Vision,” 2020, pp. 128–144. doi: 10.1007/978-3-030-17795-9_10.

[39] X. Li and K. N. Plataniotis, “A Complete Color Normalization Approach to Histopathology Images Using Color Cues Computed From Saturation-Weighted Statistics,” *IEEE Trans Biomed Eng*, vol. 62, no. 7, pp. 1862–1873, Jul. 2015, doi: 10.1109/TBME.2015.2405791.

[40] M. Macenko *et al.*, “A method for normalizing histology slides for quantitative analysis,” in *2009 IEEE International Symposium on Biomedical Imaging: From Nano to Macro*, IEEE, Jun. 2009, pp. 1107–1110. doi: 10.1109/ISBI.2009.5193250.

[41] F. Bukenya, “A hybrid approach for stain normalisation in digital histopathological images,” *Multimed Tools Appl*, vol. 79, no. 3–4, pp. 2339–2362, Jan. 2020, doi: 10.1007/s11042-019-08262-0.

[42] S. M. Butler, G. I. Webb, and R. A. Lewis, “A case study in feature invention for breast cancer diagnosis using X-ray scatter images,” in *AI 2003: Advances in Artificial Intelligence: 16th Australian Conference on AI, Perth, Australia, December 3-5, 2003. Proceedings 16*, 2003, pp. 677–685.

[43] S. D. Roy, S. Das, D. Kar, F. Schwenker, and R. Sarkar, “Computer Aided Breast Cancer Detection Using Ensembling of Texture and Statistical Image Features,” *Sensors*, vol. 21, no. 11, p. 3628, May 2021, doi: 10.3390/s21113628.

[44] X. Liu and Z. Zeng, “A new automatic mass detection method for breast cancer with false positive reduction,” *Neurocomputing*, vol. 152, pp. 388–402, Mar. 2015, doi: 10.1016/j.neucom.2014.10.040.

[45] P. K. Sethy, C. Pandey, M. R. Khan, S. K. Behera, K. Vijaykumar, and S. Panigrahi, “A cost-effective computer-vision based breast cancer diagnosis,” *Journal of Intelligent & Fuzzy Systems*, vol. 41, no. 5, pp. 5253–5263, Nov. 2021, doi: 10.3233/JIFS-189848.

[46] M. Kowal, P. Filipczuk, A. Obuchowicz, J. Korbicz, and R. Monczak, “Computer-aided diagnosis of breast cancer based on fine needle biopsy microscopic images,” *Comput Biol Med*, vol. 43, no. 10, pp. 1563–1572, Oct. 2013, doi: 10.1016/j.compbiomed.2013.08.003.

[47] S. Reis *et al.*, “Automated Classification of Breast Cancer Stroma Maturity From Histological Images,” *IEEE Trans Biomed Eng*, vol. 64, no. 10, pp. 2344–2352, Oct. 2017, doi: 10.1109/TBME.2017.2665602.

[48] Y. Zhang, B. Zhang, F. Coenen, and W. Lu, “Breast cancer diagnosis from biopsy images with highly reliable random subspace classifier ensembles,” *Mach Vis Appl*, vol. 24, no. 7, pp. 1405–1420, Oct. 2013, doi: 10.1007/s00138-012-0459-8.

[49] D. O. Tambasco Bruno, M. Z. do Nascimento, R. P. Ramos, V. R. Batista, L. A. Neves, and A. S. Martins, “LBP operators on curvelet coefficients as an algorithm to describe texture in breast cancer tissues,” *Expert Syst Appl*, vol. 55, pp. 329–340, Aug. 2016, doi: 10.1016/j.eswa.2016.02.019.

[50] N. C. Mhala and S. H. Bhandari, “Improved approach towards classification of histopathology images using bag-of-features,” in *2016 International Conference on Signal and Information Processing (IConSIP)*, IEEE, Oct. 2016, pp. 1–5. doi: 10.1109/ICONSIP.2016.7857472.

[51] L. D. True, “Morphometric applications in anatomic pathology,” *Hum Pathol*, vol. 27, no. 5, pp. 450–467, May 1996, doi: 10.1016/S0046-8177(96)90089-1.

[52] K. R. and N. K., “Automated Diagnosis of Breast Cancer Using Wavelet Based Entropy Features,” in *2018 Second International Conference on Electronics, Communication and Aerospace Technology (ICECA)*, IEEE, Mar. 2018, pp. 274–279. doi: 10.1109/ICECA.2018.8474739.

[53] M. A. Aswathy and M. Jagannath, “An SVM approach towards breast cancer classification from H&E-stained histopathology images based on integrated features,” *Med Biol Eng Comput*, vol. 59, no. 9, pp. 1773–1783, Sep. 2021, doi: 10.1007/s11517-021-02403-0.

[54] M. B. H. Thuy and V. T. Hoang, “Fusing of deep learning, transfer learning and gan for breast cancer histopathological image classification,” in *Advanced Computational Methods for Knowledge Engineering: Proceedings of the 6th International Conference on Computer Science, Applied Mathematics and Applications, ICCSAMA 2019 6*, 2020, pp. 255–266.

[55] M. Toğaçar, K. B. Özkurt, B. Ergen, and Z. Cömert, “BreastNet: A novel convolutional neural network model through histopathological images for the diagnosis of breast cancer,” *Physica A: Statistical Mechanics and its Applications*, vol. 545, p. 123592, May 2020, doi: 10.1016/j.physa.2019.123592.

[56] F. A. Spanhol, L. S. Oliveira, C. Petitjean, and L. Heutte, “Breast cancer histopathological image classification using Convolutional Neural Networks,” in *2016 International Joint Conference on Neural Networks (IJCNN)*, IEEE, Jul. 2016, pp. 2560–2567. doi: 10.1109/IJCNN.2016.7727519.

[57] Shallu and R. Mehra, “Breast cancer histology images classification: Training from scratch or transfer learning?,” *ICT Express*, vol. 4, no. 4, pp. 247–254, Dec. 2018, doi: 10.1016/j.icte.2018.10.007.

[58] A.-A. Nahid, M. A. Mehrabi, and Y. Kong, “Histopathological Breast Cancer Image Classification by Deep Neural Network Techniques Guided by Local Clustering,” *Biomed Res Int*, vol. 2018, pp. 1–20, 2018, doi: 10.1155/2018/2362108.

[59] A.-A. Nahid and Y. Kong, “Histopathological Breast-Image Classification Using Local and Frequency Domains by Convolutional Neural Network,” *Information*, vol. 9, no. 1, p. 19, Jan. 2018, doi: 10.3390/info9010019.

[60] S. Saxena, S. Shukla, and M. Gyanchandani, “Pre-trained convolutional neural networks as feature extractors for diagnosis of breast cancer using histopathology,” *Int J Imaging Syst Technol*, vol. 30, no. 3, pp. 577–591, Sep. 2020, doi: 10.1002/ima.22399.

[61] M. Gour, S. Jain, and T. Sunil Kumar, “Residual learning based CNN for breast cancer histopathological image classification,” *Int J Imaging Syst Technol*, vol. 30, no. 3, pp. 621–635, Sep. 2020, doi: 10.1002/ima.22403.

[62] K. George, S. Faziludeen, P. Sankaran, and P. Joseph K, “Breast cancer detection from biopsy images using nucleus guided transfer learning and belief based fusion,” *Comput Biol Med*, vol. 124, p. 103954, Sep. 2020, doi: 10.1016/j.compbiomed.2020.103954.

[63] Q. A. Al-Haija and A. Adebanjo, “Breast Cancer Diagnosis in Histopathological Images Using ResNet-50 Convolutional Neural Network,” in *2020 IEEE International IOT, Electronics and Mechatronics Conference (IEMTRONICS)*, IEEE, Sep. 2020, pp. 1–7. doi: 10.1109/IEMTRONICS51293.2020.9216455.

[64] R. Karthik, R. Menaka, and M. V. Siddharth, “Classification of breast cancer from histopathology images using an ensemble of deep multiscale networks,” *Biocybern Biomed Eng*, vol. 42, no. 3, pp. 963–976, Jul. 2022, doi: 10.1016/j.bbe.2022.07.006.

[65] M. A. Wakili *et al.*, “Classification of Breast Cancer Histopathological Images Using DenseNet and Transfer Learning,” *Comput Intell Neurosci*, vol. 2022, pp. 1–31, Oct. 2022, doi: 10.1155/2022/8904768.

[66] Ü. Budak, Z. Cömert, Z. N. Rashid, A. Şengür, and M. Çıbuk, “Computer-aided diagnosis system combining FCN and Bi-LSTM model for efficient breast cancer detection from histopathological images,” *Appl Soft Comput*, vol. 85, p. 105765, Dec. 2019, doi: 10.1016/j.asoc.2019.105765.

[67] H. Zerouaoui and A. Idri, “Deep hybrid architectures for binary classification of medical breast cancer images,” *Biomed Signal Process Control*, vol. 71, p. 103226, Jan. 2022, doi: 10.1016/j.bspc.2021.103226.

[68] K. George, S. Faziludeen, P. Sankaran, and J. K. Paul, “Deep Learned Nucleus Features for Breast Cancer Histopathological Image Analysis based on Belief Theoretical Classifier Fusion,” in *TENCON 2019 - 2019 IEEE Region 10 Conference (TENCON)*, IEEE, Oct. 2019, pp. 344–349. doi: 10.1109/TENCON.2019.8929539.

[69] G. Li *et al.*, “Pathological image classification via embedded fusion mutual learning,” *Biomed Signal Process Control*, vol. 79, p. 104181, Jan. 2023, doi: 10.1016/j.bspc.2022.104181.

[70] F.-Z. Nakach, H. Zerouaoui, and A. Idri, “Hybrid deep boosting ensembles for histopathological breast cancer classification,” *Health Technol (Berl)*, vol. 12, no. 6, pp. 1043–1060, Nov. 2022, doi: 10.1007/s12553-022-00709-z.

[71] S. Singh and R. Kumar, “Breast cancer detection from histopathology images with deep inception and residual blocks,” *Multimed Tools Appl*, vol. 81, no. 4, pp. 5849–5865, Feb. 2022, doi: 10.1007/s11042-021-11775-2.

[72] Y. Song, J. J. Zou, H. Chang, and W. Cai, “Adapting fisher vectors for histopathology image classification,” in *2017 IEEE 14th International Symposium on Biomedical Imaging (ISBI 2017)*, IEEE, Apr. 2017, pp. 600–603. doi: 10.1109/ISBI.2017.7950592.

[73] Z. Han, B. Wei, Y. Zheng, Y. Yin, K. Li, and S. Li, “Breast Cancer Multi-classification from Histopathological Images with Structured Deep Learning Model,” *Sci Rep*, vol. 7, no. 1, p. 4172, Jun. 2017, doi: 10.1038/s41598-017-04075-z.

[74] M. Jannesari *et al.*, “Breast Cancer Histopathological Image Classification: A Deep Learning Approach,” in *2018 IEEE International Conference on Bioinformatics and Biomedicine (BIBM)*, IEEE, Dec. 2018, pp. 2405–2412. doi: 10.1109/BIBM.2018.8621307.

[75] M. Z. Alom, C. Yakopcic, Mst. S. Nasrin, T. M. Taha, and V. K. Asari, “Breast Cancer Classification from Histopathological Images with Inception Recurrent Residual Convolutional Neural Network,” *J Digit Imaging*, vol. 32, no. 4, pp. 605–617, Aug. 2019, doi: 10.1007/s10278-019-00182-7.

[76] Y. Zhou, C. Zhang, and S. Gao, “Breast Cancer Classification From Histopathological Images Using Resolution Adaptive Network,” *IEEE Access*, vol. 10, pp. 35977–35991, 2022, doi: 10.1109/ACCESS.2022.3163822.

[77] G. Murtaza, L. Shuib, G. Mujtaba, and G. Raza, “Breast Cancer Multi-classification through Deep Neural Network and Hierarchical Classification Approach,” *Multimed Tools Appl*, vol. 79, no. 21–22, pp. 15481–15511, Jun. 2020, doi: 10.1007/s11042-019-7525-4.

[78] C. A. Ferreira *et al.*, “Classification of Breast Cancer Histology Images Through Transfer Learning Using a Pre-trained Inception Resnet V2,” 2018, pp. 763–770. doi: 10.1007/978-3-319-93000-8_86.

[79] S. Kumar and S. Sharma, “Sub-classification of invasive and non-invasive cancer from magnification independent histopathological images using hybrid neural networks,” *Evol Intell*, vol. 15, no. 3, pp. 1531–1543, Sep. 2022, doi: 10.1007/s12065-021-00564-3.

[80] D. Bardou, K. Zhang, and S. M. Ahmad, “Classification of Breast Cancer Based on Histology Images Using Convolutional Neural Networks,” *IEEE Access*, vol. 6, pp. 24680–24693, 2018, doi: 10.1109/ACCESS.2018.2831280.

[81] T. Wan, J. Cao, J. Chen, and Z. Qin, “Automated grading of breast cancer histopathology using cascaded ensemble with combination of multi-level image features,” *Neurocomputing*, vol. 229, pp. 34–44, Mar. 2017, doi: 10.1016/j.neucom.2016.05.084.

[82] Y. Zheng *et al.*, “Histopathological Whole Slide Image Analysis Using Context-Based CBIR,” *IEEE Trans Med Imaging*, vol. 37, no. 7, pp. 1641–1652, Jul. 2018, doi: 10.1109/TMI.2018.2796130.

[83] A. A. Alhussan *et al.*, “Classification of Breast Cancer Using Transfer Learning and Advanced Al-Biruni Earth Radius Optimization,” *Biomimetics*, vol. 8, no. 3, p. 270, Jun. 2023, doi: 10.3390/biomimetics8030270.

[84] P. Rani, R. Kumar, A. Jain, R. Lamba, R. Kumar Sachdeva, and T. Choudhury, “PCA-DNN: A Novel Deep Neural Network Oriented System for Breast Cancer Classification,” *EAI Endorsed Trans Pervasive Health Technol*, vol. 9, Oct. 2023, doi: 10.4108/eetpht.9.3533.

[85] L. Liu *et al.*, “Collaborative Transfer Network for Multi-Classification of Breast Cancer Histopathological Images,” *IEEE J Biomed Health Inform*, pp. 1–12, 2023, doi: 10.1109/JBHI.2023.3283042.

[86] M. A. Al-antari, S.-M. Han, and T.-S. Kim, “Evaluation of deep learning detection and classification towards computer-aided diagnosis of breast lesions in digital X-ray mammograms,” *Comput Methods Programs Biomed*, vol. 196, p. 105584, Nov. 2020, doi: 10.1016/j.cmpb.2020.105584.

[87] Y. Zhang, B. Zhang, F. Coenen, J. Xiao, and W. Lu, “Erratum to: One-class kernel subspace ensemble for medical image classification,” *EURASIP J Adv Signal Process*, vol. 2015, no. 1, p. 88, Dec. 2015, doi: 10.1186/s13634-015-0274-2.

[88] S. Tummala, J. Kim, and S. Kadry, “BreaST-Net: Multi-Class Classification of Breast Cancer from Histopathological Images Using Ensemble of Swin Transformers,” *Mathematics*, vol. 10, no. 21, p. 4109, Nov. 2022, doi: 10.3390/math10214109.

[89] A. Baccouche, B. Garcia-Zapirain, C. Castillo Olea, and A. S. Elmaghraby, “Breast Lesions Detection and Classification via YOLO-Based Fusion Models,” *Computers, Materials & Continua*, vol. 69, no. 1, pp. 1407–1425, 2021, doi: 10.32604/cmc.2021.018461.

[90] P. Kaur, G. Singh, and P. Kaur, “Intellectual detection and validation of automated mammogram breast cancer images by multi-class SVM using deep learning classification,” *Inform Med Unlocked*, vol. 16, p. 100239, 2019, doi: 10.1016/j.imu.2019.100239.

[91] F. A. Spanhol, L. S. Oliveira, C. Petitjean, and L. Heutte, “A Dataset for Breast Cancer Histopathological Image Classification,” *IEEE Trans Biomed Eng*, vol. 63, no. 7, pp. 1455–1462, Jul. 2016, doi: 10.1109/TBME.2015.2496264.